iScience

CellPress
OPEN ACCESS

Article

IL-21-armored B7H3 CAR-iNKT cells exert potent antitumor effects

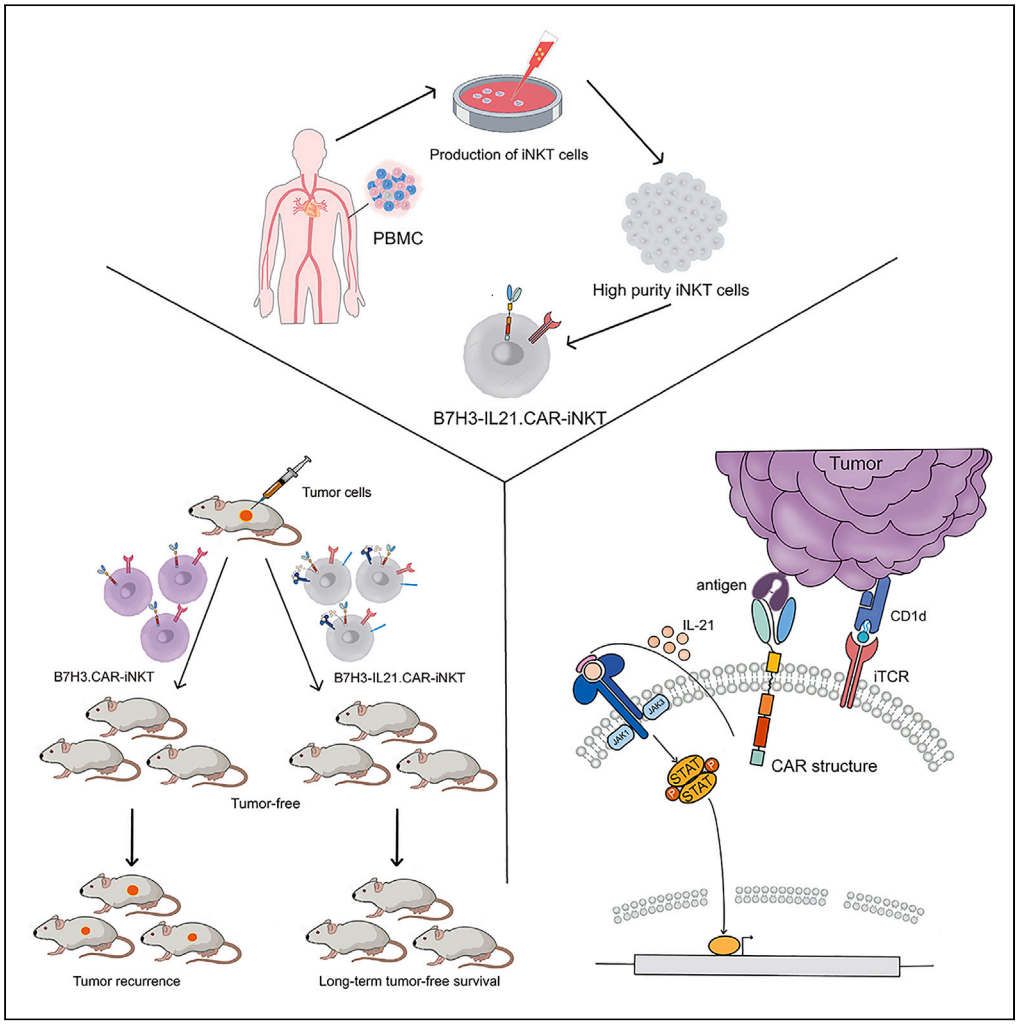

Yilin Liu, Yuanyuan Dang, Chuhan Zhang, ..., Gang Wang, Junnian Zheng, Huizhong Li

wangg@xzhmu.edu.cn (G.W.)
jnzheng@xzhmu.edu.cn (J.Z.)
lhz@xzhmu.edu.cn (H.L.)

Highlights

Addition of IL-4, GM-CSF, and IL-21 promotes *ex vivo* expansion of human iNKT

Ex vivo expanded iNKT and CAR-modified iNKT cells showed great anti-tumor activity

IL-21 armoring improved CAR-iNKT persistence and therapeutic efficacy in tumor model

Liu et al., iScience *27*, 108597
January 19, 2024
https://doi.org/10.1016/j.isci.2023.108597

iScience

CellPress
OPEN ACCESS

Article

IL-21-armored B7H3 CAR-iNKT cells exert potent antitumor effects

Yilin Liu,[1] Yuanyuan Dang,[1] Chuhan Zhang,[1] Liu Liu,[1] Wenhui Cai,[1] Liantao Li,[1,2,3] Lin Fang,[1,2,3] Meng Wang,[1,2,3] Shunzhe Xu,[1] Gang Wang,[1,2,3,*] Junnian Zheng,[2,3,*] and Huizhong Li[1,2,3,4,*]

SUMMARY

CD1d-restricted invariant NKT (iNKT) cells play a critical role in tumor immunity. However, the scarcity and limited persistence restricts their development and clinical application. Here, we demonstrated that iNKT cells could be efficiently expanded using modified cytokines combination from peripheral blood mononuclear cells. Introduction of IL-21 significantly increased the frequency of CD62L-positive memory-like iNKT cells. iNKT cells armoring with B7H3-targeting second generation CAR and IL-21 showed potent tumor cell killing activity. Moreover, co-expression of IL-21 promoted the activation of Stat3 signaling and reduced the expression of exhaustion markers in CAR-iNKT cells *in vitro*. Most importantly, IL-21-arming significantly prolonged B7H3 CAR-iNKT cell proliferation and survival *in vivo*, thus improving their therapeutic efficacy in mouse renal cancer xerograph models without observed cytokine-related adverse events. In summary, these results suggest that B7H3 CAR-iNKT armored with IL-21 is a promising therapeutic strategy for cancer treatment.

INTRODUCTION

Chimeric antigen receptor (CAR)-mediated anti-tumor strategy is a novel immunotherapy approach that currently focuses on the expression of receptors for specific tumor antigens.[1] Despite the breakthroughs CAR-T cell therapy have achieved in malignant hematological diseases,[2] there are still some barriers restrict its universal application, including the limited infiltration in solid tumor tissues,[3] suppressive tumor microenvironment,[4] and immunological challenges of allogeneic application.[5] Since the approved CAR-T therapeutics are produced by autologous T cells, which are time-consuming and cost-unfriendly, it is difficult to implement for patients with insufficient or incompetent lymphocytes.[6,7] The application of universal CAR-T cells could greatly reduce the costs and waiting time, however, their therapeutic efficacy in clinical trials is still unsatisfactory. Moreover, multiple gene editing to generate universal CAR-T might raise safety issues.[8–10] Therefore, using non-MHC-restricted innate lymphocytes to develop universal CAR-T products has become an attractive strategy.

Invariant NKT (iNKT) cells comprise a specialized subpopulation of T cells that express the semi-invariant T cell receptor (TCR) and recognize glycolipids presented on non-polymorphic CD1d molecules.[11] Contrary to MHC-restricted T cells, in autologous or allogeneic therapeutic applications, the potential GvHD of iNKT cells is constrained by the limited expression of the non-peptide glycosylation presenting CD1d protein.[12,13] iNKT cells are involved in innate immunity and rapidly produce a large array of cytokines/chemokines that influence adaptive immune in the treatment of inflammation and tumors.[14,15] The infiltration of iNKT cells into tumors is positively correlated with patients' prognosis in multiple tumors, and they may serve as a highly effective cellular platform for CAR-mediated immunotherapy.[16] CD19-specific CAR-iNKT cells had shown a stronger antitumor effect for B-cell malignancy in a preclinical study as compare to CD19 CAR-T cells due to their CAR- and CD1d-dependent double-killing mechanism.[17] Moreover, CAR-iNKT against solid tumor antigens, such as GD2[18] and CSPG4,[19] had also shown encouraging results[20] in several preclinical studies and clinical trials.

Due to the low frequency of iNKT cells in humans, a method was developed herein for the production of iNKT cells through cytokine cocktail and glycolipid antigen activation *ex vivo* from peripheral or cord blood-derived mononuclear cells. For preclinical and clinical testing, the iNKT cells obtained through the induction maintained a robust expansion. Although the memory phenotype of iNKT cell is still unknown,[21] CD62L is thought to maintain the memory-like characteristics of iNKT cells,[22] which has a potent anti-tumor reaction.[23] However, the frequency of CD62L-positive iNKT cells was not significantly increased under the initial induction protocol.

The cytokine receptor γ chain (γc) family is one of the most widely studied cytokines, including IL-2, IL-4, IL-7, IL-9, IL-15, and IL-21, which jointly promote the development of various immune cell populations and regulate cell differentiation.[24] $CD62L^{+}$ iNKT cell has high levels of IL-7R and IL-21R mRNA expression according to immunogenetic analyses of iNKT cell subpopulations.[22] IL-21 plays a significant role in the regulation of both innate and adaptive immunity by encouraging the T cell synthesis of Th1-type cytokines[23,25] and maintaining

[1]Cancer Institute, Xuzhou Medical University, 209 Tongshan Road, Xuzhou, Jiangsu 221004, China
[2]Center of Clinical Oncology, the Affiliated Hospital of Xuzhou Medical University, 99 West Huaihai Road, Xuzhou, Jiangsu 221002, China
[3]Jiangsu Center for the Collaboration and Innovation of Cancer Biotherapy, Cancer Institute, Xuzhou Med-ical University, 209 Tongshan Road, Xuzhou, Jiangsu 221004, China
[4]Lead contact
*Correspondence: wangg@xzhmu.edu.cn (G.W.), jnzheng@xzhmu.edu.cn (J.Z.), lhz@xzhmu.edu.cn (H.L.)
https://doi.org/10.1016/j.isci.2023.108597

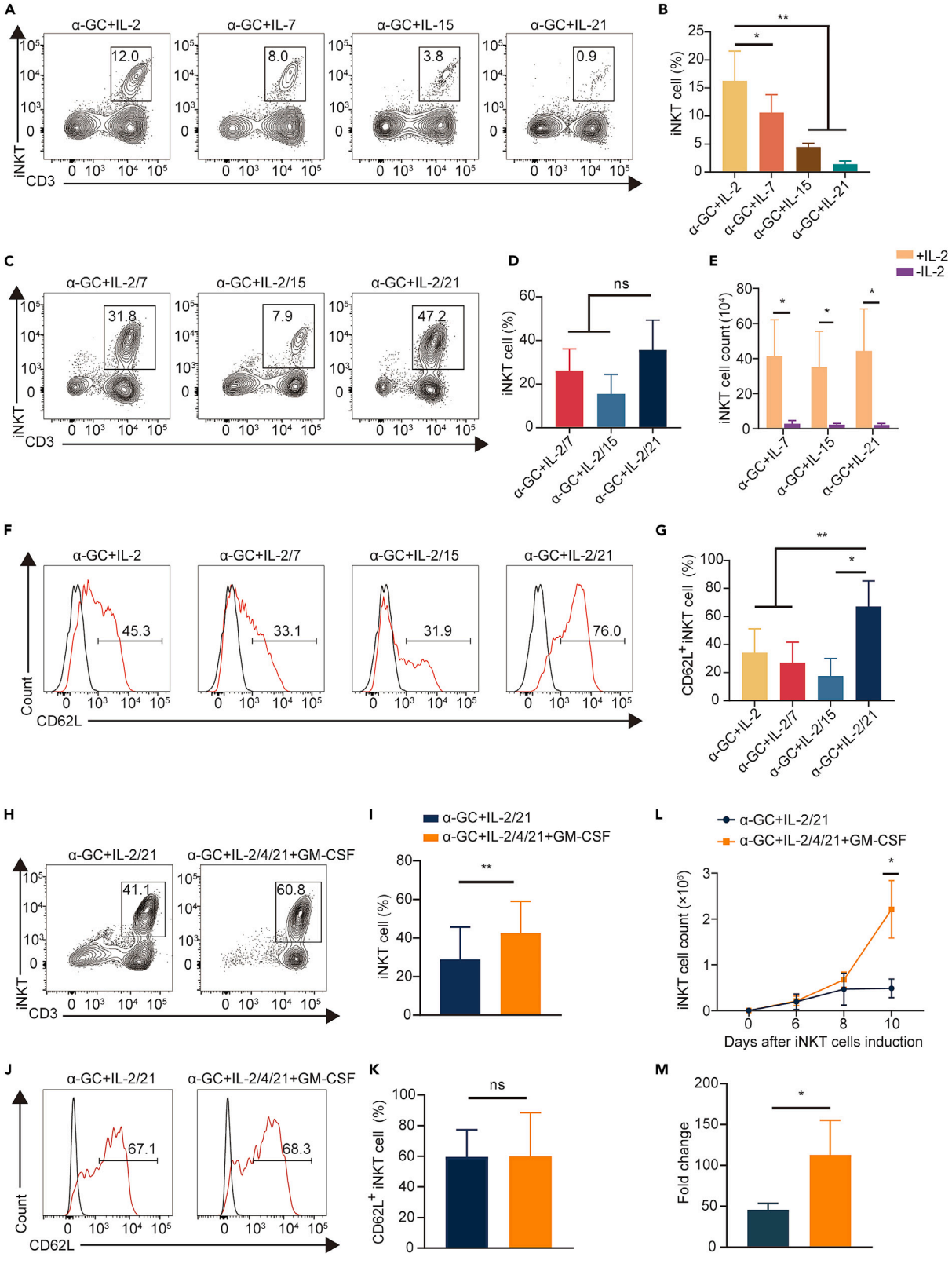
A
α-GC+IL-2
α-GC+IL-7
α-GC+IL-15
α-GC+IL-21
12.0
8.0
3.8
0.9
iNKT
CD3
B
iNKT cell (%)
α-GC+IL-2
α-GC+IL-7
α-GC+IL-15
α-GC+IL-21
C
α-GC+IL-2/7
α-GC+IL-2/15
α-GC+IL-2/21
31.8
7.9
47.2
D
iNKT cell (%)
ns
E
+IL-2
-IL-2
iNKT cell count (10⁴)
F
45.3
33.1
31.9
76.0
Count
CD62L
G
CD62L⁺ iNKT cell (%)
H
α-GC+IL-2/4/21+GM-CSF
41.1
60.8
I
L
iNKT cell count (×10⁶)
Days after iNKT cells induction
J
67.1
68.3
K
M
Fold change

Figure 1. Screening for the optimal conditions to obtain CD62L$^+$iNKT cells

(A and B) Frequency of iNKT cells on day 8 in the presence of α-GalCer (α-Gc) and multiple cytokines (IL-2, IL-7, IL-15, and IL-21), as determined by flow cytometry analysis and based on the statistical chart (α-Gc+IL-2 vs. α-Gc+IL-7: p = 0.0114, α-Gc+IL-2 vs. α-Gc+IL-15: p = 0.0084, α-Gc+IL-2 vs. α-Gc+IL-21: p = 0.0060, Student's paired t-test. Data are presented as the mean ± SD, n = 4).

(C and D) Flow cytometry analysis and statistical charts of α-Gc+IL-2/7, α-Gc+IL-2/15 and α-Gc+IL-2/21 induced iNKT cells on days 8 (NS: not significant, Student's paired t-test. Data are presented as the mean ± SD, n = 4).

(E) The number of iNKT cells induced by the combined use of cytokines compared to the single cytokine treated group (α-Gc+IL-2 vs. α-Gc+IL-2/7: p = 0.033, α-Gc+IL-2 vs. α-Gc+IL-2/15: p = 0.0491, α-Gc+IL-2 vs. α-Gc+IL-2/21: p = 0.0384, Student's paired t-test. Data are presented as the mean ± SD, n = 4).

(F and G) CD62L expression of iNKT cells was examined using flow cytometry on induction days 8 (α-Gc+IL-2 vs. α-Gc+IL-2/21: p = 0.0029, α-Gc+IL-2/7 vs. α-Gc+IL-2/21: p = 0.0025, α-Gc+IL-2/15 vs. α-Gc+IL-2/21: p = 0.0346, Student's paired t-test. Data are presented as the mean ± SD, n = 4).

(H and I) Flow cytometry analysis and statistical charts of α-Gc+IL-2/21 and α-Gc+IL-2/4/21+GM-CSF induced the frequency of iNKT cells on day 8 (α-Gc+IL-2/21 vs. α-Gc+IL-2/4/21+GM-CSF: p = 0.0013, Student's paired t-test. Data are presented as the mean ± SD, n = 4).

(J and K) The proportion of CD62L$^+$iNKT cells by α-Gc+IL-2/21 and α-Gc+IL-2/4/21+GM-CSF as determined using flow cytometry analysis and statistical charts on day 8 (NS: not significant, Student's paired t-test. Data are presented as the mean ± SD, n = 4).

(L and M) Counting statistics of iNKT cells expansion absolute numbers under the settings of α-Gc+IL-2/21 and α-Gc+IL-2/4/21+GM-CSF. (Day10: α-Gc+IL-2/21 vs. α-Gc+IL-2/4/21+GM-CSF, p = 0.0153, Fold change: α-Gc+IL-2/21 vs. α-Gc+IL-2/4/21+GM-CSF, p = 0.0130, Student's paired t-test. Data are presented as the mean ± SD, n = 4).

CD8$^+$ memory T cell production.[26] Similarly, IL-7 can promote the survival of CD4$^+$ T cell and enhance anti-tumor immunity.[27,28] Accordingly, in the present study, the initial induction system was optimized by including additional γc family cytokines. Our results showed that the addition of IL-21, but not IL-7 or IL-15, significantly enhanced the frequency of CD62L$^+$ iNKT cell during induction. Then, the ability of IL-21-armored B7H3.CAR construct to enhance the anti-tumor activity of iNKT cells was determined. Upon antigen stimulation, we found that ectopic IL-21 expression led to an increase of Stat3 phosphorylation and a decrease of exhaustion markers in CAR-iNKT cells. In addition, co-expression of IL-21 prolonged the persistence of CAR-iNKT cells and improved their therapeutic efficacy without obvious toxicity according to the results in multiple preclinical tumor models. Overall, an optimization preparation strategy for clinical CAR-iNKT cells was explored, and an alternative cellular immune platform was provided for the clinical exploration of solid tumors.

RESULT

Presence of IL-21 increases the frequency of CD62L-positive naive iNKT cells

Adoptive cell therapy by using *ex vivo* expanded iNKT cells is an attractive approach for the treatment of patients with cancer. However, obtaining clinical-scale homogeneous Th1-polarized iNKT cells with prolonged persistence remains a great challenge. The optimal conditions for the generation of high-purity iNKT cells were determined, and a memory-like phenotype of iNKT cells was ensured by examining the frequency of iNKT cells using various combinations of γc family factors and the iNKT cell agonist alpha-galactosylceramide (αGC) in different protocols. First, the induction efficiency of iNKT was compared by single cytokines, and the results showed that exposure of IL-2 elevated the percentage of iNKT cells in αGC-pulsed peripheral blood mononuclear cell (PBMC) (Figures 1A and 1B). Then, different combinations of cytokines were screened, and no significant difference was observed in the percentage of iNKT cells between different combination groups (Figures 1C and 1D). However, the number of iNKT cells induced by combined usage of cytokines indeed increased as compared with single cytokine treated groups (Figure 1E). The frequency of iNKT cells with a central memory phenotype was preserved during expansion, and the results show that IL-21 upregulated the expression of CD62L on iNKT cells, but not IL-2, IL-7, and IL-15 (Figures 1F and 1G). Through preliminary comparison, the basic conditions for iNKT cell frequency and memory phenotype, including αGc, IL-2, and IL-21, were determined.

CD1d molecules can be expressed on antigen-presenting cells, especially dendritic cells (DCs).[29] IL-4 and GM-CSF were added to the basal protocol, which still increased the iNKT cell frequency without affecting CD62L expression (Figures 1H, 1K, S1A, and S1B) and dramatically promoted iNKT cell proliferation in the late induction period (Figures 1L and 1M). Based on the results of paired comparisons, IL-21 also preserved the Th1-type chemokine receptors CCR5 and CXCR3 (Figures S1C and S1F) and the initial CD4/8 ratio of iNKT cells (Figures S1G and S1H), which were represent potentially increased cytotoxic effects and excellent tissue infiltration ability.[30] Next, iNKT cells were purified using flow cytometry sorter and over 97% purity of iNKT were obtained and activated by CD3/28 antibodies to their expansion (Figures S2A and S2B). Thereafter, the amplified iNKT cells were frozen for conservation and thawed for re-activation and -expansion. In the presence of IL-7 and IL-15 in culture medium after CD3/28 antibodies-dependent activation preserved their viability and proliferation ability of iNKT cells (Figures S2C and S2D).

Ectopic expression of IL-21 in CAR-iNKT cells improves the percentage of CD62L-positive cells

Retroviral constructs were generated, including a B7H3-specific scFv, human CD8a-derived hinge and transmembrane domains, a human CD28 costimulatory endodomain, and a human CD3ζ signaling domain (Figure 2A). The human IL-21 sequence was inserted into the B7H3.CAR construct following a 2A peptide sequence. Flow cytometry assay demonstrated that ectopic expression of IL-21 did not affect CAR transducing efficacy (Figures 2B and 2C). Then, kidney cancer cell line 786-O was confirmed to high express B7H3 antigen (Figure 2D). Upon antigen exposure, IL-21 secretion was increased in both B7H3.CAR-iNKT and B7H3-IL21.CAR-iNKT cells, and higher IL-21 expression level was found in B7H3-IL21.CAR-iNKT cells (Figure 2E). Notably, CAR-iNKT cells co-expressing IL-21 could effectively maintain CD62L$^+$ naive phenotype during their expansion, suggesting that IL-21 is benefit to sustain the naive phenotype during the iNKT induction and expansion processes (Figures 2F and 2G).

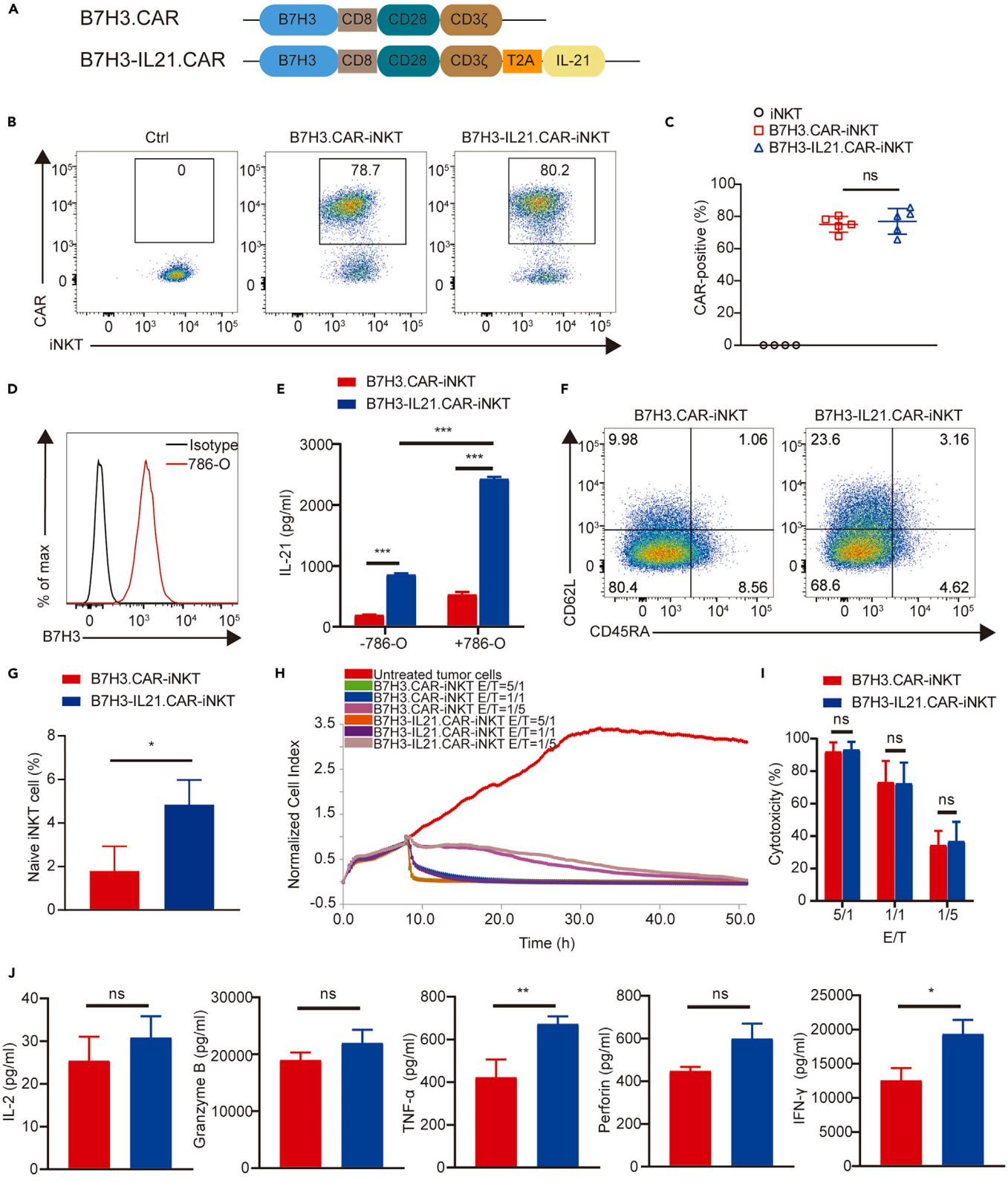
A
B7H3.CAR
B7H3
CD8
CD28
CD3ζ
B7H3-IL21.CAR
T2A
IL-21
B
Ctrl
B7H3.CAR-iNKT
B7H3-IL21.CAR-iNKT
0
78.7
80.2
CAR
iNKT
C
iNKT
B7H3.CAR-iNKT
B7H3-IL21.CAR-iNKT
ns
CAR-positive (%)
D
Isotype
786-O
% of max
B7H3
E
B7H3.CAR-iNKT
B7H3-IL21.CAR-iNKT
IL-21 (pg/ml)
***
-786-O
+786-O
F
B7H3.CAR-iNKT
B7H3-IL21.CAR-iNKT
9.98
1.06
80.4
8.56
23.6
3.16
68.6
4.62
CD62L
CD45RA
G
B7H3.CAR-iNKT
B7H3-IL21.CAR-iNKT
Naive iNKT cell (%)
*
H
Untreated tumor cells
B7H3.CAR-iNKT E/T=5/1
B7H3.CAR-iNKT E/T=1/1
B7H3.CAR-iNKT E/T=1/5
B7H3-IL21.CAR-iNKT E/T=5/1
B7H3-IL21.CAR-iNKT E/T=1/1
B7H3-IL21.CAR-iNKT E/T=1/5
Normalized Cell Index
Time (h)
I
B7H3.CAR-iNKT
B7H3-IL21.CAR-iNKT
ns
Cytotoxicity (%)
5/1
1/1
1/5
E/T
J
IL-2 (pg/ml)
Granzyme B (pg/ml)
TNF-α (pg/ml)
Perforin (pg/ml)
IFN-γ (pg/ml)
ns
**
*

Figure 2. Functional assay of CAR-iNKT cells generated by the induction system

(A) Schematic of retroviral constructs encoding B7H3.CAR with and without IL21.

(B and C) CAR expression in iNKT cells transduced (on day 3 after stimulation with CD3/28 antibody) as determined using retroviral vectors containing the indicated B7H3.CAR constructs as measured by flow cytometry (NS: not significant, Student's paired t-test. Data are presented as the mean ± SD, n = 5).

(D) Representative flow cytometric analysis of B7H3 on 786-O cell.

(E) ELISA assessment of IL-21 releases from B7H3.CAR-iNKT and B7H3-IL21.CAR-iNKT cells cultured alone or at a 1:1 E:T ratio with B7H3-positive 786-O cells stimulated for 24h (B7H3.CAR-iNKT without 786-O vs. B7H3-IL21.CAR-iNKT without 786-O: $p < 0.001$, B7H3.CAR-iNKT with 786-O vs. B7H3-IL21.CAR-iNKT with 786-O: $p < 0.001$, B7H3-IL21.CAR-iNKT without 786-O vs. B7H3-IL21.CAR-iNKT with 786-O: $p < 0.001$, Student's paired t-test. Data are presented as the mean ± SD, n = 3).

(F and G) Representative flow cytometry analysis of CD62L expression on CAR-iNKT cells with or without IL-21 on day 7 after transduction (B7H3.CAR-iNKT vs. B7H3-IL21.CAR-iNKT: $p = 0.0298$, Student's paired t-test. Data are presented as the mean ± SD, n = 3).

(H and I) Graph of the real-time cell analysis results that show the cytotoxic effect of B7H3.CAR-iNKT cells with or without IL-21 against renal cells 786-O after co-culture for 50 h at E:T ratios of 5:1, 1:1, and 1:5 (NS: not significant, Student's paired t-test. Data are presented as the mean ± SD, n = 3).

(J) iNKT and B7H3.CAR-iNKT cells with or without IL-21 were stimulated by 786-O cell, supernatants were collected after 24 h, and concentrations of the indicated cytokines were quantified using a multi-analyte flow assay kit (NS: not significant, TNF-α: B7H3.CAR-iNKT vs. B7H3-IL21.CAR-iNKT, $p = 0.0091$, IFN-γ: B7H3.CAR-iNKT vs. B7H3-IL21.CAR-iNKT, $p = 0.0128$, Student's unpaired t-test. Data are presented as the mean ± SD, n = 3).

Next, whether the expansion conditions and presence of CAR affected the killing ability of iNKT cells was determined through intrinsic CD1d-iTCR-mediated killing assay. In this process, wild-type $CD1d^{-}B7H3^{+}$ DU145 cells were synthesized to express CD1d and B7H3 singly or double-positive or double-negative (Figure S3A). One of the most well-researched iNKT cell ligands, α-GalCer, can be presented by CD1d molecules to activate iNKT cells.[31] In comparison with the control group, the presence of α-GalCer contributed to the cytotoxic effect of iNKT and CAR-iNKT cells on $CD1d^{+}$ DU145 cells, suggesting that IL-21 did not alter the activating process of CAR-iNKT cells by CD1d-dependent pathway. However, tumor killing of CAR-iNKT cells was hardly seen in CD1d and B7H3 double-negative tumor cells, emphasizing the specificity of B7H3 target (Figures S3B and S3E). These findings demonstrated that IL-21 co-expressing and CAR-iNKT preparation system was successfully established.

IL-21 enhances the reactivity of CAR-iNKT cells *in vitro*

The effectiveness of CAR-mediated iNKT cells against tumor cells *in vitro* was examined using luciferase (Ffluc)-expressing $B7H3^{+}$ 786-O as target cell. Ectopic expression of IL-21 did not affect the expansion and anti-tumor ability of CAR-iNKT cells, as determined using Real-time Cellular Analysis (RTCA) at the effector-to-target ratios of 5/1, 1/1, and 1/5 (Figures 2H, 2I, and S4A). Although all the target tumor cells were eliminated, OSRC-2 cells were less sensitive to CAR-iNKT cells than 786-O cells (Figures S4B and S4C). Moreover, B7H3-IL21.CAR-iNKT was prone to generate Th1-type cytokines in response to B7H3-positive tumor cells. The lack of notable cytokine release from untransduced iNKT cells when co-cultured with B7H3-positive tumor cells indicates the process that mediated weak antitumor activity. Notably, the co-expression of IL-21 facilitated the increased production of anti-tumor factors, including TNF-α and IFN-γ (Figure 2J).

Then, the critical components of the IL-21-mediated pro-survival signaling pathway were assessed to further confirm whether IL-21 plays a significant role in maintaining cell proliferation. The phosphorylation of Stat3 in CAR-iNKT cells co-expressing IL-21 was significantly increased, which is consistent with the IL-21-mediated T cell signaling pathway.[32] Additionally, the CAR-iNKT cells co-expressing IL-21 but not CAR-iNKT cells showed slightly activation of Stat5, indicating that IL-21 might exert a pro-survival role in the CAR-iNKT system (Figure 3A). In the absence of cytokines, CAR-iNKT cells were more prone to apoptosis than cells co-expressing IL-21, which may be the difference mediated by IL-21 (Figures 3B and 3C). In a four-round tumor cells challenge assay, we found that co-expression of IL-21 successfully delayed the exhaustion of CAR-iNKT cells after the second-round tumor cells challenge by inhibiting the expression of exhaustion markers such as LAG-3, Tim-3, and PD-1 (Figure 3D). More importantly, the results showed that IL-21 mediated more robust CAR-iNKT cell expansion (Figure 3E). Therefore, co-expression of IL-21 decreased the frequency of exhausted CAR-iNKT cells and might be attributed to the survival of effector cells in the suppressive tumor environment.

CAR-iNKT cells co-expressing IL-21 have superior persistence *in vivo*

To evaluate their persistence *in vivo*, iNKT cells were engineered with luciferase and then adoptively transferred into NCG mice bearing 786-*O*-established lung metastatic tumor (Figure 4A). The results showed that co-expression of IL-21 greatly increased the persistence of iNKT cells (Figures 4B and 4C). The frequency of iNKT cells in mouse peripheral blood was detected, and the result was consistent with that of the *in vivo* imaging system (IVIS, Figure 4D). Then, the residual iNKT cells and tumor cells in the lungs were determined. IL-21 maintained a significantly higher number of iNKT cells than the other groups (Figure 4E), while the frequency of tumor cells in the lungs of the iNKT cells treated group was approximately 10 times higher than that in IL-21 co-expressing group (Figure 4F). In addition, mice treated with B7H3-IL21.-CAR-iNKT cells had more iNKT cells in the spleens (Figure 4G). Therefore, IL-21-mediated maintenance of CAR-iNKT cells *in vivo* is consistent with *in vitro* experiments.

CAR-iNKT cells co-expressing IL-21 have superior therapeutic activity in mice

The *in vivo* CAR-iNKT cells with or without IL-21 were examined against kidney cancer. Briefly, twelves-days later after subcutaneous injection of 786-O cells, the tumor volume was approximately 80–100 mm^3. Subsequently, CAR-iNKT cells with or without IL-21 were injected through the tail

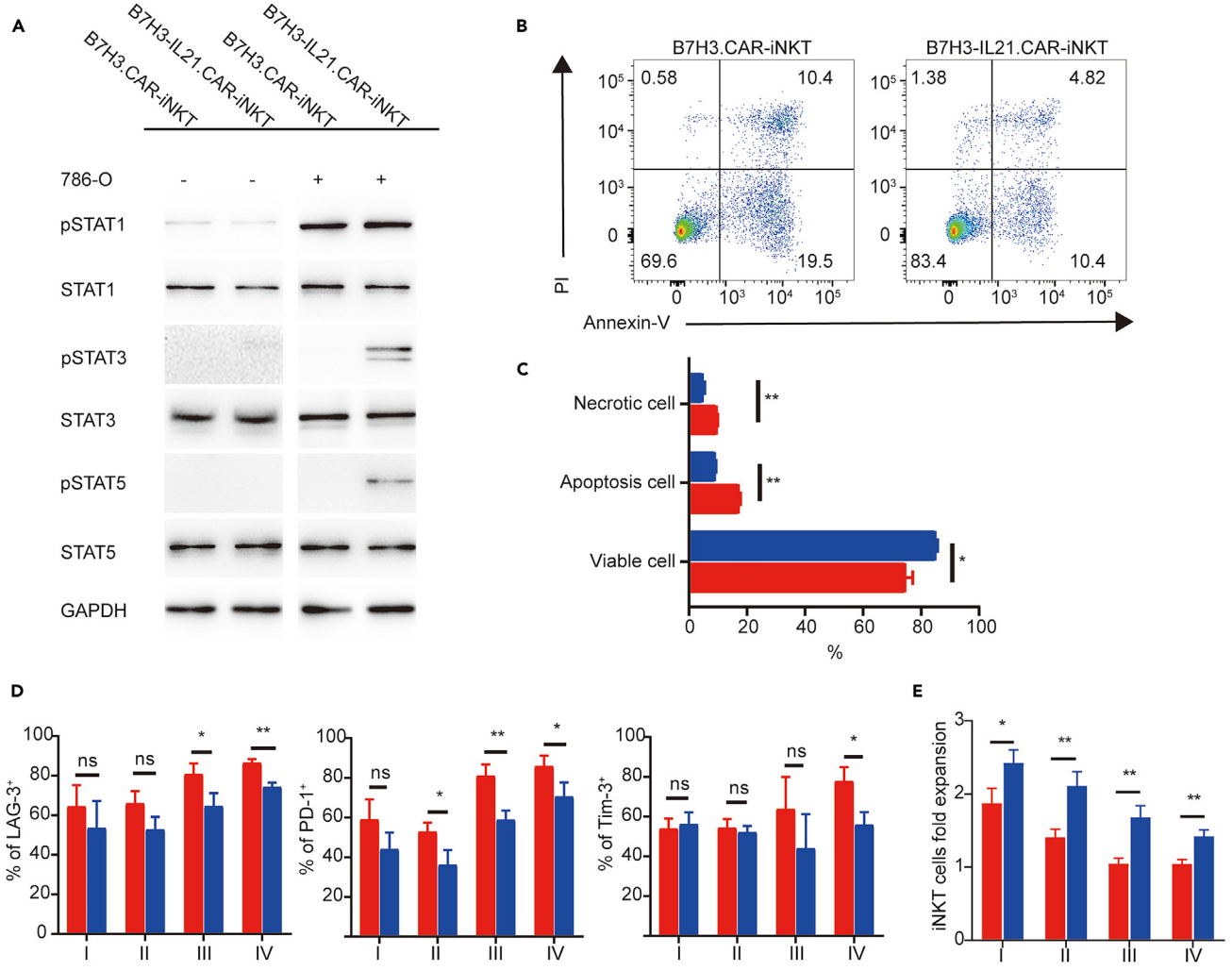

Figure 3. Functional assessment of B7H3.CAR-iNKT cells co-expressing IL21 *in vitro*

(A) Western blot analysis of the level of STAT1, STAT3, and STAT5 and the expression of phosphorylated STAT1 (pSTAT1), phosphorylated STAT3 (pSTAT3), and phosphorylated STAT5 (pSTAT5) in B7H3.CAR-iNKT and B7H3-IL21.CAR-iNKT cells co-cultured with or without 786-O cell.

(B and C) B7H3.CAR-iNKT and B7H3-IL21.CAR-iNKT cells were stained with annexin-V and PI and cultured alone in complete medium without cytokine for 2 days. PI-positive/Annexin-V-positive cells were considered as necrotic cells, PI-negative/Annexin-V-positive cells were considered as apoptosis cells, and PI-negative/Annexin-V-negative cells were considered as viable cells, which were assessed by flow cytometry and represented as histograms (Necrotic cell: B7H3.CAR-iNKT vs. B7H3-IL21.CAR-iNKT, $p = 0.0084$, Apoptosis cell: B7H3.CAR-iNKT vs. B7H3-IL21.CAR-iNKT, $p = 0.0025$, Viable cell: B7H3.CAR-iNKT vs. B7H3-IL21.CAR-iNKT, $p = 0.0271$, Student's paired t-test. Data are presented as the mean ± SD, n = 3).

(D and E) B7H3.CAR-iNKT and B7H3-IL21.CAR-iNKT cells were counted and evaluated for the expression of the exhaustion markers after each round of tumor stimulation (NS: not significant, % of LAG-3$^+$: B7H3.CAR-iNKT vs. B7H3-IL21.CAR-iNKT (III), $p = 0.0311$, B7H3.CAR-iNKT vs. B7H3-IL21.CAR-iNKT (IV), $p = 0.0022$, % of PD-1$^+$: B7H3.CAR-iNKT vs. B7H3-IL21.CAR-iNKT (II), $p = 0.0317$, B7H3.CAR-iNKT vs. B7H3-IL21.CAR-iNKT (III), $p = 0.0068$, B7H3.CAR-iNKT vs. B7H3-IL21.CAR-iNKT (IV), $p = 0.041$, % of Tim-3$^+$: B7H3.CAR-iNKT vs. B7H3-IL21.CAR-iNKT (IV), $p = 0.017$, iNKT cells fold expansion: B7H3.CAR-iNKT vs. B7H3-IL21.CAR-iNKT (I), $p = 0.0252$, B7H3.CAR-iNKT vs. B7H3-IL21.CAR-iNKT (II), $p = 0.0056$, B7H3.CAR-iNKT vs. B7H3-IL21.CAR-iNKT (III), $p = 0.0037$, B7H3.CAR-iNKT vs. B7H3-IL21.CAR-iNKT (IV), $p = 0.004$, Student's unpaired t-test. Data are presented as the mean ± SD, n = 3).

vein on day 12 and 18, respectively (Figure 5A). The mice receiving saline served as the control group. In comparison with control group or B7H3.CAR-iNKT cells treated group, B7H3-IL21.CAR-iNKT cells could consistently suppress tumor growth (Figure 5B). Three weeks following therapy, peripheral blood from mice in each group were analyzed to determine whether IL-21 was successful in preserving CAR-iNKT cells viability *in vivo* (Figure 5C). B7H3-IL21.CAR-iNKT cells exhibited a similar expansion period without IL-21 treatment group, but IL-21 supported CAR-iNKT cells with a greater proliferation. Considering the rapid progression and invasiveness of the tumor models during the observation period, differences were not observed in the survival between the groups, while weight loss was more obvious in the control group (Figure 5D).

For the visualization of the efficiency of CAR-iNKT cells against tumors *in vivo*, metastatic kidney tumor models were developed using luciferase-expressing 786-O cells. The tumor-bearing mice were divided into three groups at day 14 and treated with CAR-iNKT or

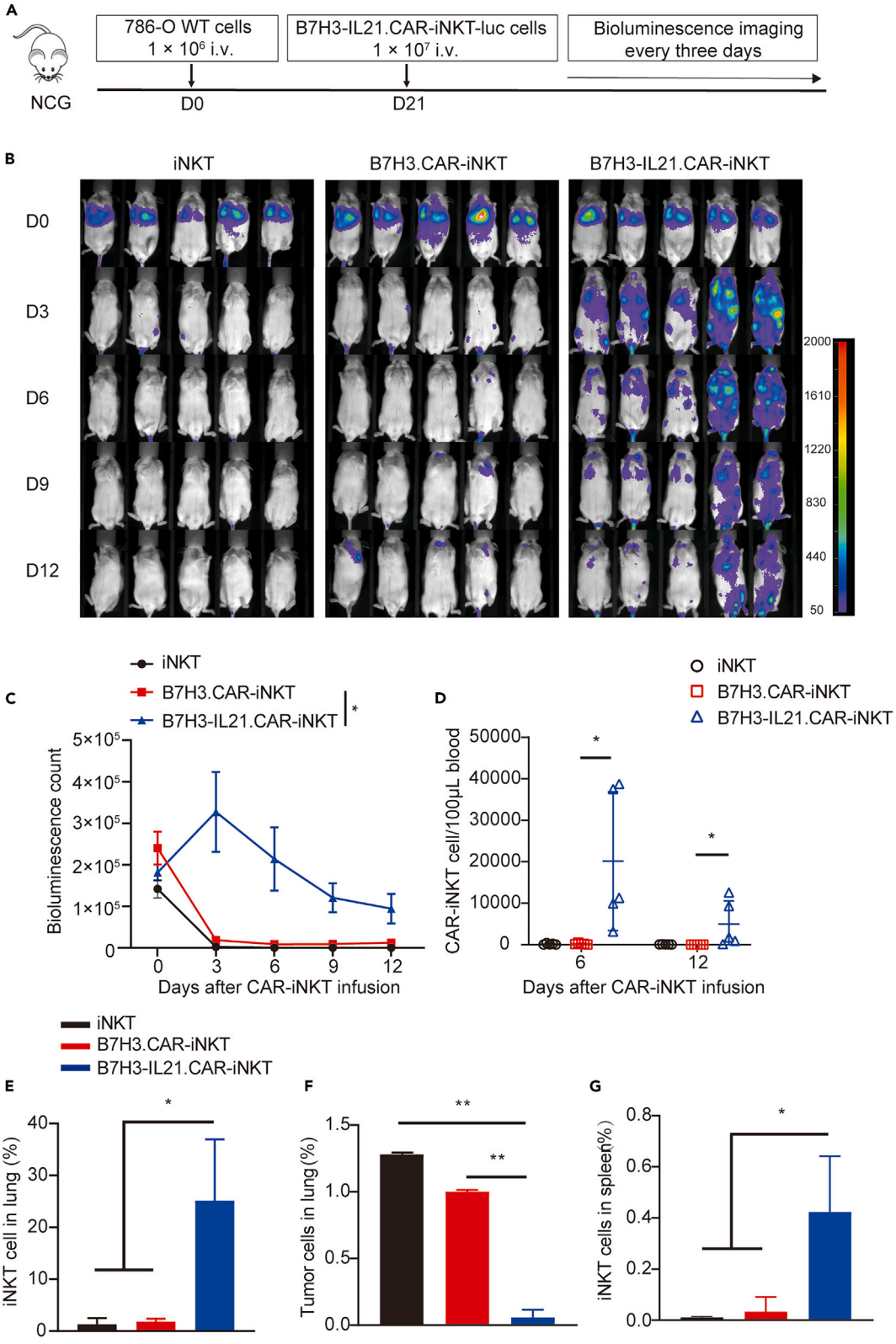
A
786-O WT cells
1 × 10^6 i.v.
B7H3-IL21.CAR-iNKT-luc cells
1 × 10^7 i.v.
Bioluminescence imaging
every three days
NCG
D0
D21
B
iNKT
B7H3.CAR-iNKT
B7H3-IL21.CAR-iNKT
D0
D3
D6
D9
D12
2000
1610
1220
830
440
50
C
iNKT
B7H3.CAR-iNKT
B7H3-IL21.CAR-iNKT
Bioluminescence count
Days after CAR-iNKT infusion
D
CAR-iNKT cell/100μL blood
Days after CAR-iNKT infusion
E
iNKT cell in lung (%)
F
Tumor cells in lung(%)
G
iNKT cells in spleen(%)

Figure 4. IL-21 significantly prolonged the survival of CAR-iNKT cells in solid tumor-bearing mice

(A) Overview of *in vivo* evaluation scheme for B7H3-IL-21.CAR-iNKT cells persistence. NSG mice were injected intravenously with 1×10^6 786-O renal tumor cell and then with 1×10^7 B7H3.CAR-iNKT cells with or without IL-21. iNKT cells were tracked by bioluminescence imaging every 3 days after treatment.

(B) Bioluminescent monitoring of iNKT, B7H3.CAR-iNKT, and B7H3-IL21.CAR-iNKT cells injected into mice xenografts models of 786-O renal tumor cell (n = 5 mice).

(C) Quantification of bioluminescence images in B (B7H3.CAR-iNKT vs. B7H3-IL21.CAR-iNKT, p = 0.0394, Student's unpaired t-test. Data are presented as the mean ± SD, n = 5 mice).

(D) At days 6 and 12 following CAR-iNKT cell treatment, CAR-iNKT cells were identified by flow cytometry in the peripheral blood (Day6: B7H3.CAR-iNKT vs. B7H3-IL21.CAR-iNKT, p = 0.0287, Day12: B7H3.CAR-iNKT vs. B7H3-IL21.CAR-iNKT, p = 0.0462. one-way ANOVA. Data are presented as the mean ± SD, n = 5 mice).

(E) Quantification of iNKT (human $CD45^+/iNKT^+$) in lung total cells as determined by flow cytometry. (iNKT vs. B7H3-IL21.CAR-iNKT: p = 0.0253, B7H3.CAR-iNKT vs. B7H3-IL21.CAR-iNKT, p = 0.0269, one-way ANOVA. Data are presented as the mean ± SD, n = 3 mice).

(F) Quantification of tumor cells (human $CD45^-/B7H3^+$) in lung total cells as determined by flow cytometry. (iNKT vs. B7H3-IL21.CAR-iNKT: p = 0.0012, B7H3.CAR-iNKT vs. B7H3-IL21.CAR-iNKT, p = 0.0021, one-way ANOVA. Data are presented as the mean ± SD, n = 3 mice).

(G) Quantification of human iNKT cells in spleen total cells as determined by flow cytometry (iNKT vs. B7H3-IL21.CAR-iNKT: p = 0.0132, B7H3.CAR-iNKT vs. B7H3-IL21.CAR-iNKT, p = 0.0177, one-way ANOVA. Data are presented as the mean ± SD, n = 3 mice).

B7H3-IL21.CAR-iNKT cells (Figure 6A). The co-expression of IL-21 group consistently controlled tumor recurrence compared with the other groups (Figures 6B and 6C). After the experiment time point, the co-expressing IL-21-treated mice achieve prolonged survival in the disease-free state (Figure 6D). Meanwhile, low-frequency iNKT cells were retained in the spleen of the co-expressing IL-21 treatment group (Figure 6E). Bone marrow analysis of the treated mice revealed a limited frequency of iNKT cells, which may be necessary to protect tumor-free mice (Figure 6F). Importantly, IL-21 did not promote the unrestrained proliferation of CAR-iNKT cells *in vivo*.

To further estimate the therapeutic efficacy of CAR-iNKT, an orthotopic kidney cancer model was established by subcapsular injection of tumor cells (Figure 7A). The saline-treated mice served as control group. The mice in the CAR-iNKT cell treatment group successively relapsed from the eighth week, while the co-expression of IL-21 could maintain a long-term tumor-free status (Figures 7B and 7C). Similarly, IL-21 did not consistently promote the presence of CAR-iNKT cells *in vivo* when the tumor cells were eliminated, and a declining trend was observed, resembling that of the non-IL-21 expressing group (Figure 7D). In comparison with the control group, mice treated in B7H3-IL21.CAR-iNKT cells effectively prolonged tumor-free survival at the time of sacrifice after 10 weeks (Figure 7E). In addition, the frequency of CAR-iNKT cells detectable in peripheral blood and spleen was low (Figures 7F and 7G). Therefore, the CAR-iNKT cell treatment group co-expressing IL-21 remarkably showed potent antitumor effects in both primary and metastatic tumors.

Moreover, the effect of the co-expression of IL-21 treatment group on the safety of the mice was evaluated. The concentration of IL-21 in mice treated with B7H3-IL21.CAR-iNKT cells was undetectable at the peak of growth in mice, which is consistent with the control and CAR-iNKT treatment group. An inflammatory response was caused by CAR-iNKT cells in the lungs of mice possibly due to the vigorous proliferation of CAR-iNKT cells, whereas was no obvious cytotoxic effect was observed in other organs (Figure S5A). Therefore, CAR-iNKT cell immunotherapy may be safe in a homogeneous setting, because unlike CAR-T cells, CAR-iNKT cells do not induce GvHD.[33]

DISCUSSION

iNKT cell is considered as a promising cellular platform for CAR-mediated tumor immunotherapy as a bridge to regulate innate and adaptive immunity. Considering that the frequency of human peripheral blood iNKT cell is too low to satisfy clinical scale application, previous studies have shown that *ex vivo* expanded iNKT cell can be engineered to express tumor-specific CAR and exhibit CAR-mediated immunotherapeutic potential.[17] In the present study, the properties of iNKT cells were explored to develop an *ex vivo* expansion strategy to acquire and enhance the therapeutic efficacy of CAR-iNKT cells by co-expressing IL-21.

An approach was established for the induction of iNKT cells by αGC combined with cytokines cocktail, which can obtain high-purity and clinical-scale products from the peripheral blood of healthy donors within 3 weeks. In comparison with other iNKT cell acquiring approaches, our strategy requires only a small amount of peripheral blood and myonuclear cells. This *ex vivo* iNKT preparation strategy remarkably increases the access to iNKT cells and reduces the cost and improves the safety of CAR-iNKT cells. We found that iNKT cells prepared with our strategy could expand on average by more than 1000-fold *ex vivo*. More interestingly, we found that expanded iNKT cells could be cryopreserved and thawed to expand hundreds of times after reactivation with CD3/28 antibody, which is different from T cells and shows a much stronger expansion capacity. At present, the causes of this phenomenon remain unclear, and future studies aim to compare and analyze the characteristics of iNKT cells reactivated by different rounds. However, it is certain that iNKT cells obtained under the optimized expansion protocol after multiple-time activations still have considerable antitumor responses.

Given the lack of knowledge on how to increase the frequency of central memory-like iNKT cells in the expansion system. CD62L is thought to be a key marker for preserving the long-term survival of iNKT and T cells *in vitro*.[34] IL-2, IL-7, IL-15, and IL-21 are particularly important members of the γc-chain coreceptor family of cytokines for T cell proliferation, differentiation, and internal environment homeostasis.[35–37] *In vitro* expansion may benefit from the addition of IL-7 or IL-15 for the continuous production of $CD62L^+$ central memory iNKT cells.[18,38] Based on the induction strategies of different cytokine combinations, the frequency of single cytokine induction of iNKT cell was significantly lower than that of multi-cytokine induction protocols. Consistent with previous studies,[23] the addition of IL-21 produced a noticeably greater percentage of $CD62L^+$ iNKT cell subpopulation. In addition, the frequency of $CD62L^+$ iNKT cells is not affected following TCR activation. Meanwhile,

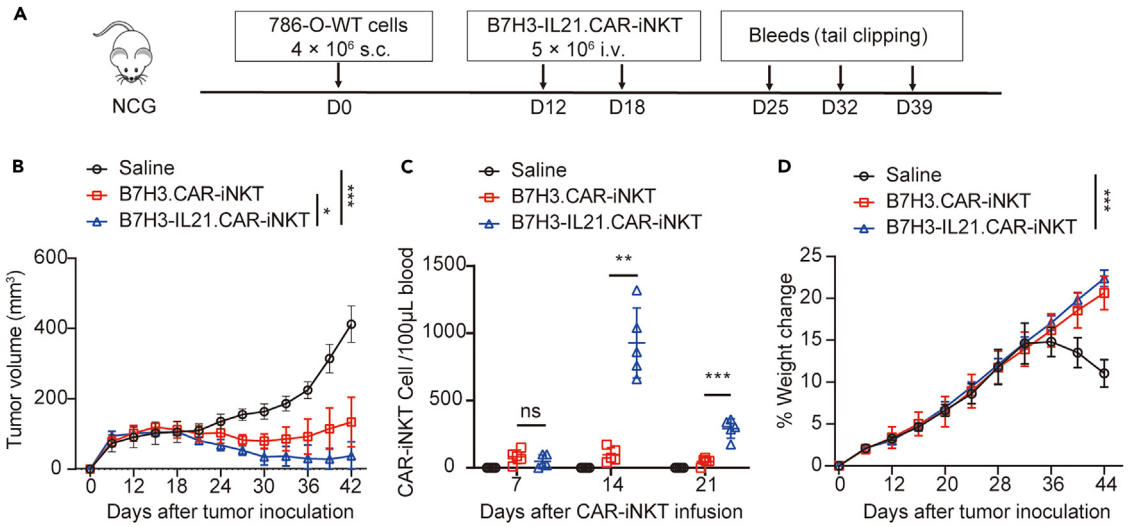

Figure 5. IL-21 promotes CAR-iNKT cells to inhibit subcutaneous tumors

(A) Schematic of *in vivo* evaluation scheme for the effectiveness of B7H3.CAR iNKT cells. NSG mice were injected subcutaneously with 4 × 10^6 786-O renal tumor cells, which was recorded as day 0. CAR-iNKT cells were administered via tail vein injection starting from the 12th day, and the body weight and tumor volume were measured every 3–4 days. For three continuous weeks following treatment, the frequency of B7H3.CAR-iNKT cells was found in the peripheral blood of NCG mice (n = 5 mice).

(B) Administration of B7H3.CAR-iNKT cells and B7H3-IL21.CAR-iNKT cells decreased the tumor volume. Data are represented as mean ± SD of five mice in each group, and statistical significance was calculated with ANOVA multiple comparison. (Saline vs. B7H3-IL21.CAR-iNKT: p = 0.0008, B7H3.CAR-iNKT vs. B7H3-IL21.CAR-iNK: p = 0.0425, one-way ANOVA. Data are presented as the mean ± SD, n = 5 mice).

(C) At days 7, 14, and 21 following treatment, CAR-iNKT cells was found by flow cytometry in the peripheral blood. (NS: not significant, Day14: B7H3.CAR-iNKT vs. B7H3-IL21.CAR-iNKT, p = 0.0046, Day21: B7H3.CAR-iNKT vs. B7H3-IL21.CAR-iNKT, p < 0.001, Student's unpaired t-test. Data are presented as the mean ± SD, n = 5 mice).

(D) Percentage change in body weight in tumor-bearing mice. Percentage weight change was calculated as: (weight at time X – weight at time 0)/(weight at time 0). (Saline vs. B7H3-IL21.CAR-iNKT: p < 0.001, Student's unpaired t-test. Data are presented as the mean ± SD, n = 5 mice).

presence of IL-21 is benefit for iNKT cell proliferation.[39] Although IL-21 induces apoptosis of DC cells, this phenomenon was prevented by adding GM-CSF without affecting the frequency of iNKT cells.[40] Previous studies in murine models have demonstrated that $CD4^-$ iNKT subset exerts more potent antitumor activity,[41] but the significant bias in the ratio of $CD4^+$ and $CD4^-$ subpopulations was not observed using our current protocol. The results indicated that the ratio of $CD4^+$ and $CD4^-$ iNKT subpopulations is closely related to the original differences among donors.

IL-21 was identified as an important cytokine in iNKT-cell-mediated immune regulation.[39] Singh. H et al. found that CAR-T cells preferentially proliferate and develop an early memory phenotype known as CD62L in the presence of IL-21,[42] which is consistent with our findings. Therefore, we sought to explore whether the combination of IL-21 and B7H3.CAR-iNKT cell could enhance the survival of CAR-iNKT and improve tumor killing efficiency. CAR-iNKT cells co-expressing IL-21 promoted the release of TNF-α and IFN-γ, but the difference in the cytotoxicity *in vitro* was not significant.

In the lung metastasis model of renal cancer in NCG mice, B7H3-IL21.CAR-iNKT treatment group significant prolonged iNKT cells persistence, especially at the site of tumorigenesis, suggesting that CAR-iNKT cells have a superior migratory capacity. Indeed, higher levels of chemokine receptors, such as CCR5 and CXCR3, were found in iNKT cells than memory T cells.[43] In addition, IL-21 promoted CAR iNKT cell survival and sustained tumor suppression in tumor-bearing mice. In the present study, IL-21 is found to improve the function of CAR-iNKT cells in tumor-bearing mice without triggering the over-expansion of CAR-iNKT cells after tumor clearance. Given the limitations of immunodeficient mice, the study was unable to authentically assess the effect of CAR-iNKT cells co-expressing IL-21 on the allogeneic immune system.

The results confirmed that IL-21 promoted the activation of CAR-iNKT cells via STAT-dependent signaling pathways. IL-21 prefers to activate Stat3-mediated cell proliferation over other cytokines of the γc-chain family.[44] Further research is currently being done on the mechanism of IL-21-driven Stat3 activation in iNKT cell. Interestingly, IL-21-mediated a slightly stronger phosphorylation of Stat5, which supports the anti-apoptotic effect of CAR-iNKT cells to some extent. Additionally, in a repeated antigen stimulation assay, CAR-iNKT cells expressing IL-21 eliminated tumor cells quickly and considerably lowered the expression of exhaustion markers. IL-21 may prevent the exhaustion of iNKT cells from terminal differentiation upon multiple antigen stimulation or T cell dysfunction in the same way.[40]

Central memory-like iNKT cell subpopulations were effectively and reliably acquired by optimizing highly reproducible strategies. The maintenance of the memory and low level of exhaustion of CAR-iNKT cells largely depend on the existence of IL-21. Moreover, the

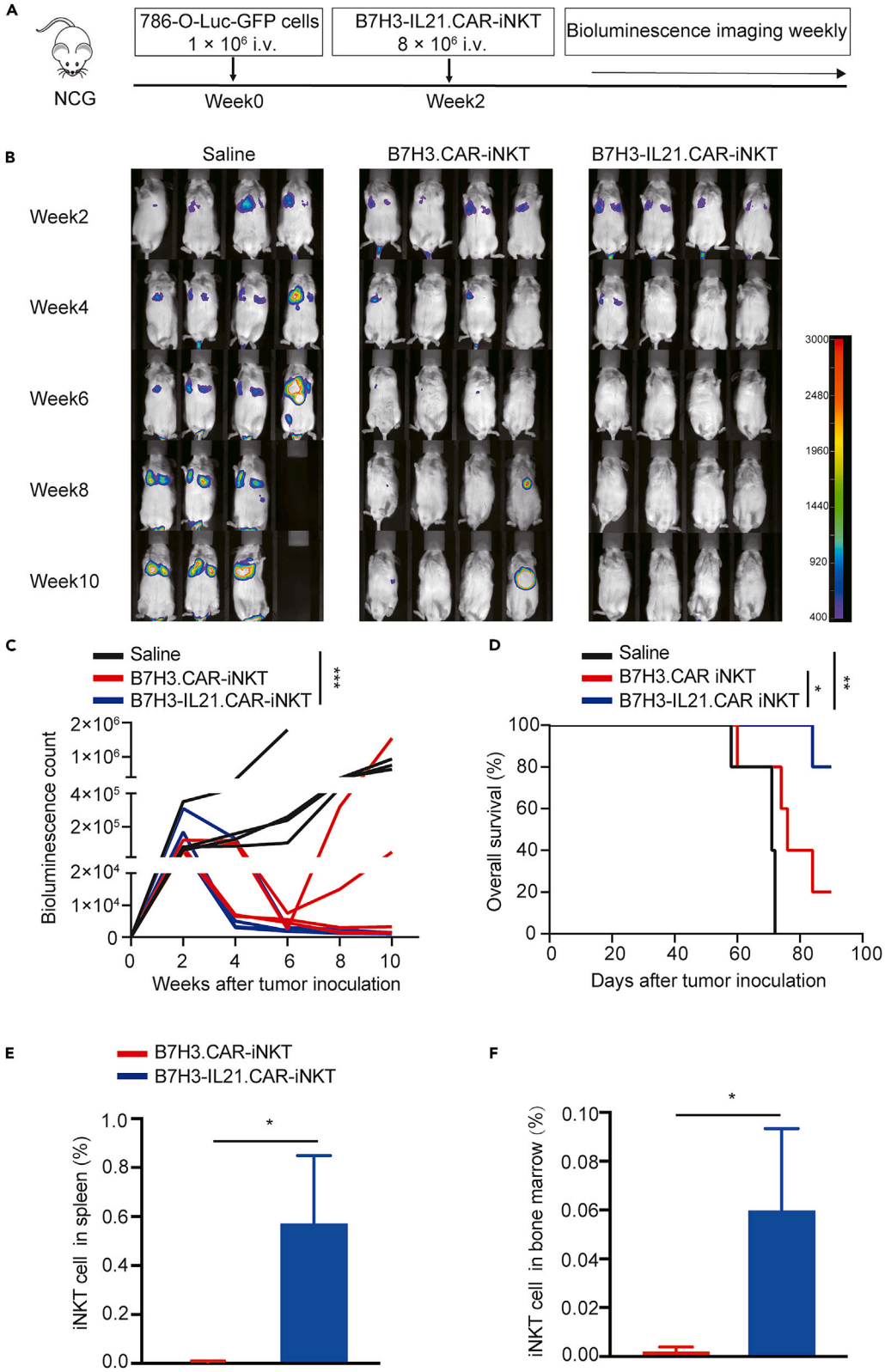
A
NCG
786-O-Luc-GFP cells
1 × 10⁶ i.v.
B7H3-IL21.CAR-iNKT
8 × 10⁶ i.v.
Bioluminescence imaging weekly
Week0
Week2
B
Saline
B7H3.CAR-iNKT
B7H3-IL21.CAR-iNKT
Week2
Week4
Week6
Week8
Week10
3000
2480
1960
1440
920
400
C
Saline
B7H3.CAR-iNKT
B7H3-IL21.CAR-iNKT
***
Bioluminescence count
2×10⁶
1×10⁶
4×10⁵
2×10⁵
2×10⁴
1×10⁴
0
0 2 4 6 8 10
Weeks after tumor inoculation
D
Saline
B7H3.CAR iNKT
B7H3-IL21.CAR iNKT
*
**
Overall survival (%)
100
80
60
40
20
0
0 20 40 60 80 100
Days after tumor inoculation
E
B7H3.CAR-iNKT
B7H3-IL21.CAR-iNKT
*
iNKT cell in spleen (%)
1.0
0.8
0.6
0.4
0.2
0.0
F
*
iNKT cell in bone marrow (%)
0.10
0.08
0.06
0.04
0.02
0.00

Figure 6. B7H3-IL21.CAR-iNKT cells exhibited excellent therapeutic activity *in vivo*

(A) Schematic representation of *in vivo* tumor challenge experiments. NSG mice were injected intravenously with 1 × 10^6 luciferase-labeled 786-O renal tumor cells and then with 8 × 10^6 B7H3.CAR-iNKT with or without IL-21 after 14 days. Tumor growth was assessed weekly by bioluminescence imaging (n = 4 mice).

(B) Bioluminescent monitoring of saline, B7H3.CAR and B7H3-IL21.CAR-iNKT cells injected into tumor mice model.

(C) Quantification of bioluminescence images in B. (Saline vs. B7H3-IL21.CAR-iNKT: $p < 0.001$, Student's unpaired t-test).

(D) Kaplan-Meier curve generated from the survival of animals in B. (Saline vs. B7H3-IL21.CAR-iNKT: $p = 0.0091$, B7H3.CAR-iNKT vs. B7H3-IL21.CAR-iNK: $p = 0.0401$, Log rank (Mantel-Cox). n = 4 mice).

(E) iNKT cells (human $CD45^+/iNKT^+$) were quantified in spleen by flow cytometry and are represented as histograms. (B7H3.CAR-iNKT vs. B7H3-IL21.CAR-iNKT: $p = 0.0247$, Student's unpaired t-test. Data are presented as the mean ± SD, n = 3 mice).

(F) iNKT cells (human $CD45^+/iNKT^+$) were quantified in bone marrow by flow cytometry and are represented as histograms. (B7H3.CAR-iNKT vs. B7H3-IL21.CAR-iNKT: $p = 0.0414$, Student's unpaired t-test. Data are presented as the mean ± SD, n = 3 mice).

co-expression of IL-21 successfully preserves effector cell survival *in vivo* to assist in tumor suppression by directly promoting the adaptability of CAR-iNKT cells and offer a preclinical experimental platform for CAR-mediated iNKT cell immunotherapy.

Limitations of the study

Although we have optimized the strategy for inducing iNKT cells to ensure the availability for clinical-level applications, notably, not all PBMC-derived cells have the potential to be induced into iNKT cells, which may depend on the factors of the donor themselves or the frequency of the initial iNKT cells and remains to be further studied. In the present study, antitumor activity of CAR-modified iNKT armoring with or without IL-21 was tested. Considering the experiments were performed in an immunodeficient mouse model, the metabolic profile of iNKT cells with high expressed IL-21 and their influences on tumor immune microenvironment should be further explored.

STAR★METHODS

Detailed methods are provided in the online version of this paper and include the following:

- KEY RESOURCES TABLE
- RESOURCE AVAILABILITY
  - Lead contact
  - Materials availability
  - Data and code availability
- EXPERIMENTAL MODEL AND SUBJECT DETAILS
  - Cell lines
  - Experimental models
- METHOD DETAILS
  - CAR constructs and retrovirus production
  - iNKT cell isolation, sorting, activation and transduction
  - Flow cytometry
  - Cytotoxicity assays
  - Multiplex cytokine quantification assay and ELISA
  - Serial tumor challenge assay
  - Western blot assay
- QUANTIFICATION AND STATISTICAL ANALYSIS

SUPPLEMENTAL INFORMATION

Supplemental information can be found online at https://doi.org/10.1016/j.isci.2023.108597.

ACKNOWLEDGMENTS

This project is supported by grants from the National Key R&D Program of China (No. 2018YFA0900900), Natural Science Key Project of Jiangsu Provincial Education Department (No. 21KJA320007), Jiangsu Province Graduate Student Scientific Research Innovation Project (Nos. KYCX21_2668 and KYCX22_2891), Jiangsu Province college students' innovation and entrepreneurship training program (No. 202110313002Z), China Postdoctoral Science Foundation (No. 2022M722680), the Youth Technology Innovation Team of Xuzhou Medical University (No. TD202003, TD202201), Jiangsu Provincial Key Medical Discipline, The Project of Invigorating Health Care through Science, Technology and Education (No. ZDXKA2016014) and the Qing Lan Project of Jiangsu Province.

AUTHOR CONTRIBUTIONS

Y.L.: Conceptualization, Experiment, Software, Data curation, Writing—Original Draft, Preparation, Writing—Review and Editing. Y.D.: Experiment, Editing. C.Z.: Experiment. L.L.: Experiment, Software. W.C.: Experiment. L.L.: Fund support. F.L.: Fund support. M.W.: Plasmid design.

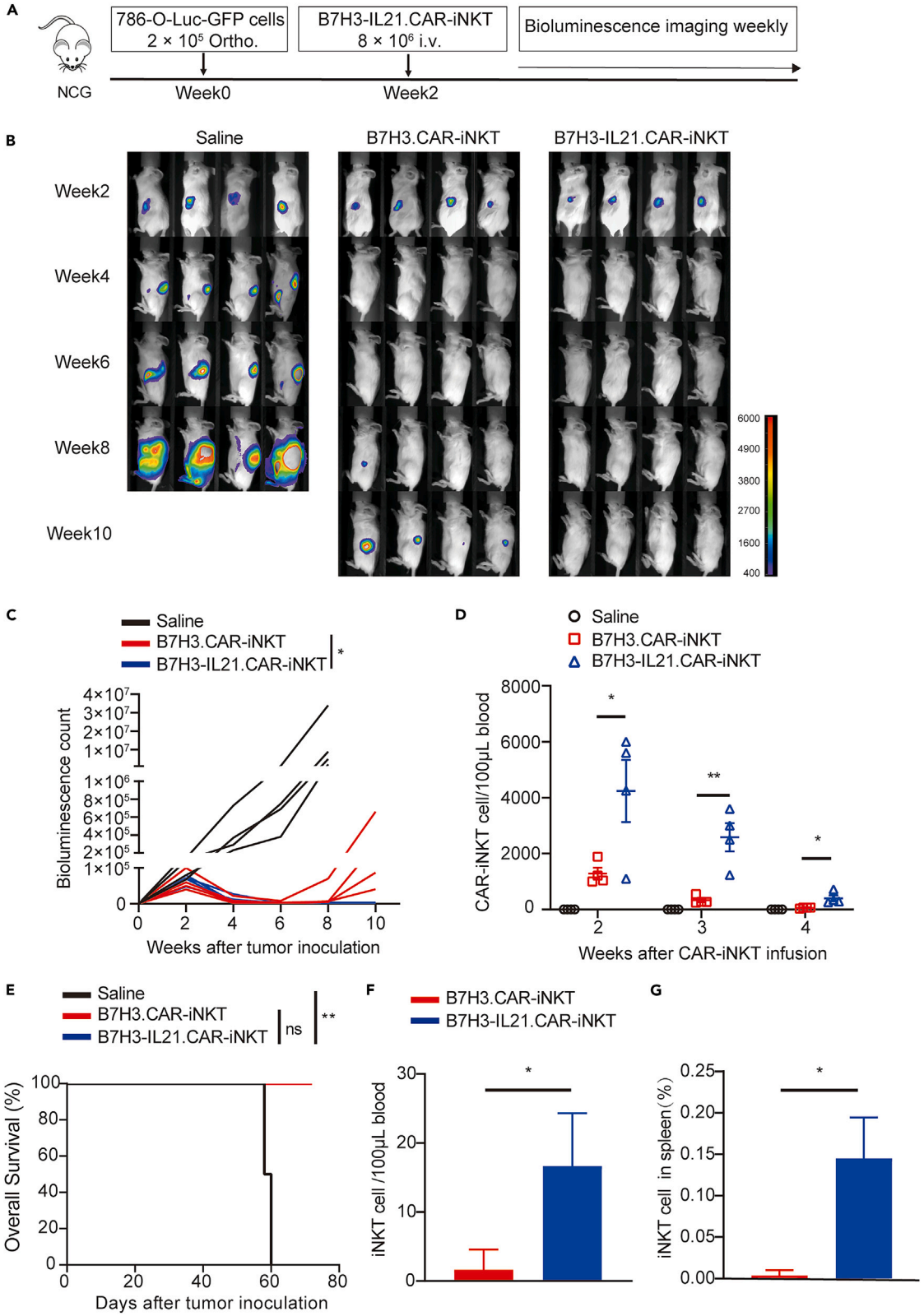
A
786-O-Luc-GFP cells
2 × 10⁵ Ortho.
B7H3-IL21.CAR-iNKT
8 × 10⁶ i.v.
Bioluminescence imaging weekly
NCG
Week0
Week2
B
Saline
B7H3.CAR-iNKT
B7H3-IL21.CAR-iNKT
Week2
Week4
Week6
Week8
Week10
6000
4900
3800
2700
1600
400
C
Saline
B7H3.CAR-iNKT
B7H3-IL21.CAR-iNKT
*
Bioluminescence count
Weeks after tumor inoculation
D
Saline
B7H3.CAR-iNKT
B7H3-IL21.CAR-iNKT
CAR-iNKT cell/100μL blood
Weeks after CAR-iNKT infusion
E
Saline
B7H3.CAR-iNKT
B7H3-IL21.CAR-iNKT
ns
**
Overall Survival (%)
Days after tumor inoculation
F
B7H3.CAR-iNKT
B7H3-IL21.CAR-iNKT
iNKT cell /100μL blood
G
iNKT cell in spleen(%)

Figure 7. Co-expression of IL-21 in CAR-iNKT treatment group effectively controlled tumor recurrence

(A) Schematic illustration of treatment process *in situ* tumor model. In total, 2×10^5 luciferase-labeled 786-O renal tumor cells were injected in the renal capsule, followed by 8×10^6 B7H3.CAR-iNKT with or without IL-21. Tumor measurement was assessed weekly by bioluminescence imaging (n = 4 mice).

(B) Bioluminescent monitoring of saline, B7H3.CAR, and B7H3-IL21.CAR-iNKT cells injected into the tumor mice models.

(C) Quantification of bioluminescence images in B (B7H3.CAR-iNKT vs. B7H3-IL21.CAR-iNKT: p = 0.0471, Student's unpaired t-test. n = 4).

(D) Assay of CAR iNKT cells in peripheral blood by flow cytometry (Week2: B7H3.CAR-iNKT vs. B7H3-IL21.CAR-iNKT, p = 0.0399, Week3: B7H3.CAR-iNKT vs. B7H3-IL21.CAR-iNKT, p = 0.0045, Week4: B7H3.CAR-iNKT vs. B7H3-IL21.CAR-iNKT, p = 0.0189, Student's unpaired t-test. Data are presented as the mean ± SD, n = 4 mice).

(E) Kaplan–Meier curve generated from survival of animals in B (NS: not significant. Saline vs. B7H3-IL21.CAR-iNKT: p = 0.0084, Log rank (Mantel-Cox). n = 4 mice).

(F) The quantification of human iNKT cells (human $CD45^+/iNKT^+$) collected from peripheral blood mononuclear cells (PBMNC) by flow cytometry (B7H3.CAR-iNKT vs. B7H3-IL21.CAR-iNKT: p = 0.0218, Student's unpaired t-test. Data are presented as the mean ± SD, n = 3 mice).

(G) The quantification of human iNKT cells (human $CD45^+/iNKT^+$) collected from spleen by flow cytometry (B7H3.CAR-iNKT vs. B7H3-IL21.CAR-iNKT: p = 0.0119, Student's unpaired t-test. Data are presented as the mean ± SD, n = 3 mice).

S.X.: Experiment. G.W.: Conceptualization, Supervision, Fund support, Writing— Review and Editing. J.Z.: Supervision, Fund support. H.L.: Conceptualization, Supervision, Fund support, Writing— Review and Editing.

DECLARATION OF INTERESTS

All other authors have no conflict of interest to declare for this research.

H.L., J.Z., G.W., Y.L., and Y.D. hold patents in this manuscript secured under the numbers 202110827989.3 and 202110783589.7.

Received: March 11, 2023
Revised: October 6, 2023
Accepted: November 28, 2023
Published: November 30, 2023

REFERENCES

1. Wagner, D.L., Fritsche, E., Pulsipher, M.A., Ahmed, N., Hamieh, M., Hegde, M., Ruella, M., Savoldo, B., Shah, N.N., Turtle, C.J., et al. (2021). Immunogenicity of CAR T cells in cancer therapy. Nat. Rev. Clin. Oncol. *18*, 379–393.
2. Cao, J., Wang, G., Cheng, H., Wei, C., Qi, K., Sang, W., Zhenyu, L., Shi, M., Li, H., Qiao, J., et al. (2018). Potent anti-leukemia activities of humanized CD19-targeted Chimeric antigen receptor T (CAR-T) cells in patients with relapsed/refractory acute lymphoblastic leukemia. Am. J. Hematol. *93*, 851–858.
3. Labanieh, L., Majzner, R.G., and Mackall, C.L. (2018). Programming CAR-T cells to kill cancer. Nat. Biomed. Eng. *2*, 377–391.
4. Quail, D.F., and Joyce, J.A. (2013). Microenvironmental regulation of tumor progression and metastasis. Nat. Med. *19*, 1423–1437.
5. Depil, S., Duchateau, P., Grupp, S.A., Mufti, G., and Poirot, L. (2020). 'Off-the-shelf' allogeneic CAR T cells: development and challenges. Nat. Rev. Drug Discov. *19*, 185–199.
6. Schuster, S.J., Svoboda, J., Chong, E.A., Nasta, S.D., Mato, A.R., Anak, Ö., Brogdon, J.L., Pruteanu-Malinici, I., Bhoj, V., Landsburg, D., et al. (2017). Chimeric Antigen Receptor T Cells in Refractory B-Cell Lymphomas. N. Engl. J. Med. *377*, 2545–2554.
7. Reddy, O.L., Stroncek, D.F., and Panch, S.R. (2020). Improving CAR T cell therapy by optimizing critical quality attributes. Semin. Hematol. *57*, 33–38.
8. Ren, J., Liu, X., Fang, C., Jiang, S., June, C.H., and Zhao, Y. (2017). Multiplex Genome Editing to Generate Universal CAR T Cells Resistant to PD1 Inhibition. Clin. Cancer Res. *23*, 2255–2266.
9. Torikai, H., Reik, A., Soldner, F., Warren, E.H., Yuen, C., Zhou, Y., Crossland, D.L., Huls, H., Littman, N., Zhang, Z., et al. (2013). Toward eliminating HLA class I expression to generate universal cells from allogeneic donors. Blood *122*, 1341–1349.
10. Georgiadis, C., Preece, R., Nickolay, L., Etuk, A., Petrova, A., Ladon, D., Danyi, A., Humphryes-Kirilov, N., Ajetunmobi, A., Kim, D., et al. (2018). Long Terminal Repeat CRISPR-CAR-Coupled "Universal" T Cells Mediate Potent Anti-leukemic Effects. Mol. Ther. *26*, 1215–1227.
11. Cohen, N.R., Garg, S., and Brenner, M.B. (2009). Antigen Presentation by CD1 Lipids, T Cells, and NKT Cells in Microbial Immunity. Adv. Immunol. *102*, 1–94.
12. Brigl, M., and Brenner, M.B. (2004). CD1: antigen presentation and T cell function. Annu. Rev. Immunol. *22*, 817–890.
13. Liu, Y., Wang, G., Chai, D., Dang, Y., Zheng, J., and Li, H. (2022). iNKT: A new avenue for CAR-based cancer immunotherapy. Transl. Oncol. *17*, 101342.
14. Lee, Y.J., Wang, H., Starrett, G.J., Phuong, V., Jameson, S.C., and Hogquist, K.A. (2015). Tissue-Specific Distribution of iNKT Cells Impacts Their Cytokine Response. Immunity *43*, 566–578.
15. Wang, H., and Hogquist, K.A. (2017). Wait, Wait . OK Now Go In: iNKT Cells Resolve Liver Inflammation. Immunity *47*, 609–610.
16. Motohashi, S., Okamoto, Y., Yoshino, I., and Nakayama, T. (2011). Anti-tumor immune responses induced by iNKT cell-based immunotherapy for lung cancer and head and neck cancer. Clin. Immunol. *140*, 167–176.
17. Rotolo, A., Caputo, V.S., Holubova, M., Baxan, N., Dubois, O., Chaudhry, M.S., Xiao, X., Goudevenou, K., Pitcher, D.S., Petevi, K., et al. (2018). Enhanced Anti-lymphoma Activity of CAR19-iNKT Cells Underpinned by Dual CD19 and CD1d Targeting. Cancer Cell *34*, 596–610.e11.
18. Xu, X., Huang, W., Heczey, A., Liu, D., Guo, L., Wood, M., Jin, J., Courtney, A.N., Liu, B., Di Pierro, E.J., et al. (2019). NKT Cells Coexpressing a GD2-Specific Chimeric Antigen Receptor and IL15 Show Enhanced In Vivo Persistence and Antitumor Activity against Neuroblastoma. Clin. Cancer Res. *25*, 7126–7138.
19. Simon, B., Wiesinger, M., März, J., Wistuba-Hamprecht, K., Weide, B., Schuler-Thurner, B., Schuler, G., Dörrie, J., and Uslu, U. (2018). The Generation of CAR-Transfected Natural Killer T Cells for the Immunotherapy of Melanoma. Int. J. Mol. Sci. *19*, 2365.
20. Heczey, A., Courtney, A.N., Montalbano, A., Robinson, S., Liu, K., Li, M., Ghatwai, N., Dakhova, O., Liu, B., Raveh-Sadka, T., et al. (2020). Anti-GD2 CAR-NKT cells in patients with relapsed or refractory neuroblastoma: an interim analysis. Nat. Med. *26*, 1686–1690.
21. Sallusto, F., Geginat, J., and Lanzavecchia, A. (2004). Central memory and effector memory T cell subsets: function, generation, and maintenance. Annu. Rev. Immunol. *22*, 745–763.
22. Tian, G., Courtney, A.N., Jena, B., Heczey, A., Liu, D., Marinova, E., Guo, L., Xu, X., Torikai, H., Mo, Q., et al. (2016). CD62L+ NKT cells have prolonged persistence and antitumor activity in vivo. J. Clin. Invest. *126*, 2341–2355.
23. Ngai, H., Tian, G., Courtney, A.N., Ravari, S.B., Guo, L., Liu, B., Jin, J., Shen, E.T., Di Pierro, E.J., and Metelitsa, L.S. (2018). IL-21 Selectively Protects CD62L(+) NKT Cells and Enhances Their Effector Functions for Adoptive Immunotherapy. J. Immunol. *201*, 2141–2153.

24. Lin, J.X., and Leonard, W.J. (2018). The Common Cytokine Receptor gamma Chain Family of Cytokines. Cold Spring Harbor Perspect. Biol. *10*, a028449.
25. Kane, A., Deenick, E.K., Ma, C.S., Cook, M.C., Uzel, G., and Tangye, S.G. (2014). STAT3 is a central regulator of lymphocyte differentiation and function. Curr. Opin. Immunol. *28*, 49–57.
26. Allard, E.L., Hardy, M.P., Leignadier, J., Marquis, M., Rooney, J., Lehoux, D., and Labrecque, N. (2007). Overexpression of IL-21 promotes massive CD8+ memory T cell accumulation. Eur. J. Immunol. *37*, 3069–3077.
27. Chetoui, N., Boisvert, M., Gendron, S., and Aoudjit, F. (2010). Interleukin-7 promotes the survival of human CD4+ effector/memory T cells by up-regulating Bcl-2 proteins and activating the JAK/STAT signalling pathway. Immunology *130*, 418–426.
28. Ding, Z.C., Habtetsion, T., Cao, Y., Li, T., Liu, C., Kuczma, M., Chen, T., Hao, Z., Bryan, L., Munn, D.H., and Zhou, G. (2017). Adjuvant IL-7 potentiates adoptive T cell therapy by amplifying and sustaining polyfunctional antitumor CD4+ T cells. Sci. Rep. *7*, 12168.
29. Gerlini, G., Hefti, H.P., Kleinhans, M., Nickoloff, B.J., Burg, G., and Nestle, F.O. (2001). Cd1d is expressed on dermal dendritic cells and monocyte-derived dendritic cells. J. Invest. Dermatol. *117*, 576–582.
30. Musha, H., Ohtani, H., Mizoi, T., Kinouchi, M., Nakayama, T., Shiiba, K., Miyagawa, K., Nagura, H., Yoshie, O., and Sasaki, I. (2005). Selective infiltration of CCR5(+)CXCR3(+) T lymphocytes in human colorectal carcinoma. Int. J. Cancer *116*, 949–956.
31. Zhang, Y., Springfield, R., Chen, S., Li, X., Feng, X., Moshirian, R., Yang, R., and Yuan, W. (2019). alpha-GalCer and iNKT Cell-Based Cancer Immunotherapy: Realizing the Therapeutic Potentials. Front. Immunol. *10*, 1126.
32. Spolski, R., and Leonard, W.J. (2008). Interleukin-21: basic biology and implications for cancer and autoimmunity. Annu. Rev. Immunol. *26*, 57–79.
33. Heczey, A., Liu, D., Tian, G., Courtney, A.N., Wei, J., Marinova, E., Gao, X., Guo, L., Yvon, E., Hicks, J., et al. (2014). Invariant NKT cells with chimeric antigen receptor provide a novel platform for safe and effective cancer immunotherapy. Blood *124*, 2824–2833.
34. Graef, P., Buchholz, V.R., Stemberger, C., Flossdorf, M., Henkel, L., Schiemann, M., Drexler, I., Höfer, T., Riddell, S.R., and Busch, D.H. (2014). Serial transfer of single-cell-derived immunocompetence reveals stemness of CD8(+) central memory T cells. Immunity *41*, 116–126.
35. Mackall, C.L., Fry, T.J., and Gress, R.E. (2011). Harnessing the biology of IL-7 for therapeutic application. Nat. Rev. Immunol. *11*, 330–342.
36. Jung, Y.W., Kim, H.G., Perry, C.J., and Kaech, S.M. (2016). CCR7 expression alters memory CD8 T-cell homeostasis by regulating occupancy in IL-7- and IL-15-dependent niches. Proc. Natl. Acad. Sci. USA *113*, 8278–8283.
37. Hinrichs, C.S., Spolski, R., Paulos, C.M., Gattinoni, L., Kerstann, K.W., Palmer, D.C., Klebanoff, C.A., Rosenberg, S.A., Leonard, W.J., and Restifo, N.P. (2008). IL-2 and IL-21 confer opposing differentiation programs to CD8+ T cells for adoptive immunotherapy. Blood *111*, 5326–5333.
38. Trujillo-Ocampo, A., Cho, H.W., Clowers, M., Pareek, S., Ruiz-Vazquez, W., Lee, S.E., and Im, J.S. (2020). IL-7 During Antigenic Stimulation Using Allogeneic Dendritic Cells Promotes Expansion of CD45RA(-)CD62L(+) CD4(+) Invariant NKT Cells With Th-2 Biased Cytokine Production Profile. Front. Immunol. *11*, 567406.
39. Coquet, J.M., Kyparissoudis, K., Pellicci, D.G., Besra, G., Berzins, S.P., Smyth, M.J., and Godfrey, D.I. (2007). IL-21 is produced by NKT cells and modulates NKT cell activation and cytokine production. J. Immunol. *178*, 2827–2834.
40. Wan, C.K., Oh, J., Li, P., West, E.E., Wong, E.A., Andraski, A.B., Spolski, R., Yu, Z.X., He, J., Kelsall, B.L., and Leonard, W.J. (2013). The cytokines IL-21 and GM-CSF have opposing regulatory roles in the apoptosis of conventional dendritic cells. Immunity *38*, 514–527.
41. Crowe, N.Y., Coquet, J.M., Berzins, S.P., Kyparissoudis, K., Keating, R., Pellicci, D.G., Hayakawa, Y., Godfrey, D.I., and Smyth, M.J. (2005). Differential antitumor immunity mediated by NKT cell subsets in vivo. J. Exp. Med. *202*, 1279–1288.
42. Singh, H., Figliola, M.J., Dawson, M.J., Huls, H., Olivares, S., Switzer, K., Mi, T., Maiti, S., Kebriaei, P., Lee, D.A., et al. (2011). Reprogramming CD19-specific T cells with IL-21 signaling can improve adoptive immunotherapy of B-lineage malignancies. Cancer Res. *71*, 3516–3527.
43. Kim, C.H., Butcher, E.C., and Johnston, B. (2002). Distinct subsets of human Valpha24-invariant NKT cells: cytokine responses and chemokine receptor expression. Trends Immunol. *23*, 516–519.
44. Zeng, R., Spolski, R., Casas, E., Zhu, W., Levy, D.E., and Leonard, W.J. (2007). The molecular basis of IL-21-mediated proliferation. Blood *109*, 4135–4142.
45. Vera, J., Savoldo, B., Vigouroux, S., Biagi, E., Pule, M., Rossig, C., Wu, J., Heslop, H.E., Rooney, C.M., Brenner, M.K., and Dotti, G. (2006). T lymphocytes redirected against the kappa light chain of human immunoglobulin efficiently kill mature B lymphocyte-derived malignant cells. Blood *108*, 3890–3897.

STAR★METHODS

KEY RESOURCES TABLE

REAGENT or RESOURCE	SOURCE	IDENTIFIER
Antibodies		
anti-human TCR Vα24-Jα18(iNKT cell) APC	BioLegend	catalog number 342908; RRID:AB_1731848
anti-human TCR Vα24-Jα18(iNKT cell) PE	BioLegend	catalog number 342904; RRID:AB_2078494
anti-human CD3 APC	BioLegend	catalog number 317318; RRID:AB_1937212
anti-human CD3 PerCP/Cyanine5.5	BioLegend	catalog number 317336; RRID:AB_2561628
anti-human CD4 FITC	BioLegend	catalog number 300506; RRID:AB_314074
anti-human CD4 APC	BioLegend	catalog number 300514; RRID:AB_314082
anti-human CD8 PE/Cyanine7	BioLegend	catalog number 344712; RRID:AB_2044008
anti-human CD8 PE	BioLegend	catalog number 344706; RRID:AB_1953244
anti-human CD45 FITC	BioLegend	catalog number 304006; RRID:AB_314394
anti-human CD45 APC	BioLegend	catalog number 304012; RRID:AB_314400
anti-human CD62L FITC	BioLegend	catalog number 304804; RRID:AB_314464
anti-human CD195 (CCR5) PerCP/Cyanine5.5	BioLegend	catalog number 359112; RRID:AB_2562964
anti-human CD195 (CCR5) APC	BioLegend	catalog number 359122; RRID:AB_2564073
anti-human CD183 (CXCR3) FITC	BioLegend	catalog number 353704; RRID:AB_10983066
anti-human CD45RA PE/Cyanine7	BioLegend	catalog number 304126; RRID:AB_10708879
anti-human CD366 (Tim-3) PE/Cyanine7	BioLegend	catalog number 345014; RRID:AB_2561720
anti-human CD366 (Tim-3) PE	BioLegend	catalog number 345006; RRID:AB_2116576
anti-human CD279 (PD-1) PE/Cyanine7	BioLegend	catalog number 367414; RRID:AB_2572165
anti-human CD223(LAG-3) PerCP/Cyanine5.5	BioLegend	catalog number 369312; RRID:AB_2629755
anti-human CD223(LAG-3) Alexa Fluor®647	BioLegend	catalog number 369304; RRID:AB_2566480
BD Pharmingen™ Mouse Anti-Human CD1d APC	BD Biosciences	catalog number 563505; RRID:AB_2738246
anti-human CD276 (B7-H3) PE	BioLegend	catalog number 331606; RRID:AB_1279197
Stat1 (D1K9Y) Rabbit mAb	Cell Signaling Technology	catalog number 14994T; RRID:AB_2737027
Stat5 (D2O6Y) Rabbit mAb	Cell Signaling Technology	catalog number 94205T; RRID:AB_2737403
Phospho-Stat1 (Tyr701) (58D6) Rabbit mAb	Cell Signaling Technology	catalog number 9167T; RRID:AB_561284
Phospho-Stat3 (Tyr705) (D3A7) XP® Rabbit mAb	Cell Signaling Technology	catalog number 9145T; RRID:AB_2491009
Phospho-Stat5 (Tyr694) (C11C5) Rabbit mAb	Cell Signaling Technology	catalog number 9359T; RRID:AB_823649
STAT1 Polyclonal antibody	Proteintech	catalog number 10144-2-AP; RRID:AB_2286875
STAT1 Monoclonal antibody	Proteintech	catalog number 66545-1-Ig; RRID:AB_2881907
GAPDH Polyclonal antibody	Proteintech	catalog number 10494-1-AP; RRID:AB_2263076
GAPDH Monoclonal antibody	Proteintech	catalog number 60004-1-Ig; RRID:AB_2107436
anti-human TCRVα24 PE	Beckman Coulter	catalog number IM2283; RRID:AB_131321
anti-human TCRVβ11 APC	Beckman Coulter	catalog number A66905
InVivoMAb anti-human/monkey CD28	Bioxcell	catalog number BE0291; RRID: AB_2687814
InVivoMab anti-human CD3	Bioxcell	catalog number BE0001-2; RRID: AB_1107632

(*Continued on next page*)

Continued

REAGENT or RESOURCE	SOURCE	IDENTIFIER
Chemicals peptides and recombinant proteins		
Dulbecco's Modified Eagle Medium(DMEM)	KeyGEN BioTECH	catalog number KGM12800N-500
Fetal Bovine Serum(Superfine)	Biochannel	catalog number BC-SE-FBS01
Gibco™Penicillin-Streptomycin	Gibco	catalog number 15140122
RPMI-1640	KeyGEN BioTECH	catalog number KGM31800-500
Iscove's Modified Dulbecco Medium(IMDM)	KeyGEN BioTECH	catalog number KGM12200-500
Gibco™GlutaMAX™ Supplement	Thermo Fisher Scientific	catalog number 35050061
Recombinant Human Interleukin-21(rHuIL-21)	PrimeGene	catalog number 101-21
α-Galactosylceramide	Funakoshi	catalog number KRN7000
Recombinant Human Interleukin-7(rHuIL-7)	PrimeGene	catalog number 101-07
Recombinant Human Interleukin-15(rHuIL-15)	PrimeGene	catalog number 101-15
Recombinant Human Interleukin-2(rHuIL-2)	PrimeGene	catalog number 101-02
Recombinant Human Interleukin-4(rHuIL-4)	PeproTech	catalog number 101-04
Recombinant Human Granulocyte-Macrophage Colony Stimulating Factor(rHuGM-CSF)	PeproTech	catalog number 102-03
X-VIVO™ 15 Serum-free Hematopoietic Cell Medium	LONZA	catalog number 04-418Q
RetroNectin-Recombinant Human Fibronectin Fragment	TAKARA	catalog number T100B
7-AAD Viability Staining Solution	BioLegend	catalog number 420404
Recombinant Human B7-H3 Fc Chimera protein	R&D System	catalog number 1027-B3-100
Alexa Fluor® 647 AffiniPure F(ab')₂ Fragment Goat Anti-Human IgG, F(ab')₂ fragment specific	Jackson ImmunoResearch Inc.	catalog number 109-606-097, RRID:AB_2337898
trypan-blue	Sigma-aldrich	catalog number T8154
RIPA lysis buffer	Beyotime	catalog number P0013C
Phosphate Buffered Saline(PBS,Powder)	Servicebio	catalog number G0002-2L
Critical commercial assays		
LEGENDplex™ Human CD8/NK Panel (13-plex) w/VbP V02	BioLegend	catalog number 741187
BCA protein assay kit	Thermo Fisher Scientific	catalog number A55864
Human IL-21 Precoated ELISA Kit	达优	catalog number 1112102
Annexin V-FITC/PI	KeyGEN BioTECH	catalog number KGA108
Experimental models: Cell lines		
786-O	ATCC	N/A
786-O-Luc	This paper	N/A
OSRC-2	ATCC	N/A
OSRC-2-Luc	This paper	N/A
DU145	ATCC	N/A
DU145-CD1d	This paper	N/A
293T	ATCC	N/A
Experimental models: Organisms/strains		
NCG mice	male	https://cn.gempharmatech.com

(*Continued on next page*)

Continued

REAGENT or RESOURCE	SOURCE	IDENTIFIER
Recombinant DNA		
SFG.B7H3.CAR-28ζ	This paper	N/A
SFG.B7H3-IL21.CAR-28ζ	This paper	N/A
Software and algorithms		
FlowJo software	FlowJo	https://www.flowjo.com/
GraphPad Prism Version 8	GraphPad Prism	https://www.graphpad.com/
Real Time Cell Analysis	RTCA	https://www.agilent.com/en/product/cell-analysis/real-time-cell-analysis
Indigo	Indigo	https://www.berthold.com/en/

RESOURCE AVAILABILITY

Lead contact

Further information on resources and reagents should be directed to the lead contact, Huizhong Li (lhz@xzhmu.edu.cn).

Materials availability

Materials generated in this study are available from the lead contact, Huizhong Li (lhz@xzhmu.edu.cn).

Data and code availability

- Any additional information required to reanalyze the data reported in this paper is available from the lead contact upon request.
- All data presented in this study will be shared upon reasonable request by the lead contact.
- This paper does not report any original code.

EXPERIMENTAL MODEL AND SUBJECT DETAILS

Cell lines

The renal cancer cell lines 786-O, 786-O^{Luc}, OSRC-2, and OSRC-2^{Luc}, prostate cancer cell lines DU145 and CD1d-positive DU145, and human embryonic kidney cell line 293T were purchased from American Type Culture Collection. OSRC-2 was cultured in Dulbecco's Modified Eagle Medium (DMEM) containing 10% FBS and 100 μg/mL penicillin/streptomycin. The renal cancer cell lines 786-O and prostate cancer cell line DU145 cell were cultured in RPMI1640 medium supplemented with 10% FBS and 100 μg/mL penicillin/streptomycin. 293T cells were maintained in IMDM supplemented with 10% FBS and 1% GlutaMAX. All cell lines were incubated at 37°C with 5% CO_2. The medium was changed every 2–3 days. Cells were kept in culture for less than 2 weeks for any given experiment.

Experimental models

Male NCG (NOD/ShiLtJGpt-Prkdc^{em26Cd52}Il2rg^{em26Cd22}/Gpt) mice were purchased from GemPharmatech (Nanjing, China), and all animal procedures and protocols (IACUC No.202009A055) were approved by the Laboratory Animal Ethical Committee of Xuzhou Medical University. The distribution of CAR-iNKT cells *in vivo* was observed by subjecting the five-week-old NCG male mice received 1×10^6 786-O cells to tail vein injection. At 21 days post tumor cell inoculation, B7H3.CAR-iNKT-Luc and B7H3-IL21.CAR-iNKT-Luc cells were injected intravenously via the tail vein (1×10^7 cells/mouse), and the cells were generated from the same donor. Thereafter, bioluminescent imaging (BLI) was performed every 3 days. The therapeutic effect of B7H3.CAR-iNKT cells was verified with and without IL-21 against renal cancer by constructing a lung metastasis model by tail vein injection of 1×10^6 firefly luciferase-labeled 786-O cells. On day 14, mice were treated with 8×10^6 CAR iNKT cells. In addition, the NCG mice kidney cancer orthotopic model was developed via subcapsule injection with 2×10^5 firefly luciferase-labeled 786-O cells. On day 14, mice were treated with 8×10^6 CAR iNKT cells. Tumor growth was assessed weekly by BLI. At the time of euthanasia, the heart, liver, spleen, lung, and kidney samples were collected and subjected to hematoxylin-eosin staining.

METHOD DETAILS

CAR constructs and retrovirus production

The vector encoding the B7H3 specific scFv, CD8α transmembrane region, CD28, and CD3ζ intracellular signal domains was used to construct B7-H3 CAR. Then, the plasmid vector that encodes the CAR in combination with the IL-21 was generated using a 2A-sequence peptide. Transient transfection of 293T cells was carried out with a CAR-containing plasmid, the RDF plasmid, and the PeqPam3 plasmid as previously described.[45] Viral supernatants were collected at 48 and 72 h post-transfection, centrifuged at 2,000 ×g for 10 min, and frozen at −80°C for future use.

iNKT cell isolation, sorting, activation and transduction

Cord blood and PBMC of healthy donors were isolated by density gradient centrifugation. iNKT cells were induced by IL-2 (50 U/ml) and α-Galcer (500 ng/mL; KRN7000) with or without IL-7 (10 ng/mL; PrimeGene), IL-15 (5 ng/mL; PrimeGene), IL-21 (10 ng/mL; PrimeGene), IL-4 (500 U/ml; PeproTech), and GM-CSF (500 U/ml; PeproTech). iNKT cells were stained with anti-iNKT (6B11) and CD3 (OKT3) antibodies and purified by FACS Aria III. The culture was supplemented every other day with IL-7 (10 ng/mL; PrimeGene) and IL-15 (5 ng/mL; PrimeGene) in complete X-VIVO (X-VIVO, 5% FBS; Gibco, 2 mM GlutaMAX; Thermo Fisher Scientific). On day 3 after stimulation with CD3/28 antibodies, 24 well non-treated culture plates were coated overnight with retronectin (TAKARA) in advance. Approximately 1 mL of retroviral supernatant was added, and the mixture was centrifuged at 2,000 ×g for 90 min and then removed. Then, 5×10^5 activated iNKT cells were seeded and centrifuged for 10 min at 1,000 ×g. iNKT cells were collected after 48 h for transduction efficiency assay and continued expansion for *in vitro* and *in vivo* experiments.

Flow cytometry

iNKT cells were subjected to phenotype analysis by flow cytometry using Abs specific to human TCR Vα24-Jα18 (6B11), CD3 (OKT3), CD4 (RPA-T4), CD8 (SK1), CD45 (HI30), CD62L (DREG-56), CCR5 (J418F1), CXCR3 (G025H7), CD45RA (HI100), Tim-3 (F38-2E2), PD-1 (NAT105), LAG-3 (11C3C65), and CD1d (CD1d42; BD Biosciences). 7-AAD viability staining solution (BioLegend) was used to distinguish between dead and living cells. Human iNKT cells were stained using PerCP/Cy5.5 mouse anti-human CD3 and PE mouse anti-human TCR Vα24-Jα18 or the combination of mouse anti-human PE-TCRVa24 (C15, Beckman Coulter) and APC-TCRVb11 (C21, Beckman Coulter). The expression of CAR was identified using recombinant human B7-H3 Fc protein (R&D system) and goat anti-human Alexa Fluor647-F(ab')$_2$ fragment (Jackson ImmunoResearch Inc.). The expression of human B7H3 on tumor cell lines was detected using anti-CD276 (DCN.70). The data were analyzed using FlowJo software (Flow V10).

Cytotoxicity assays

The cytotoxicity of effector cells was detected using real-time xCELLigence analysis (RTCA). Briefly, 50 μL of fresh complete medium (1640 and DMEM supplemented with 10% FBS) was placed in each well of the E-plate 16 (ACEA Bioscience) to obtain background impedance readings. Then, 1×10^4 786-O or OSRC-2 cells suspended in 50 μL of complete medium was added to the wells. After 30 min of incubation at room temperature, the E-plates were placed onto the RTCA SP Station located in the CO_2 incubator. After the cell index (CI) reached the plateau phase, serial dilutions of 5×10^4, 1×10^4, and 2×10^3 B7H3.CAR and B7H3-IL21.CAR-iNKT cells in 100 μL of culture medium were added to the wells. CI values were continuously measured every 15 min to reflect the cytotoxicity.

Multiplex cytokine quantification assay and ELISA

Supernatants from the co-cultures of CAR-iNKT cells with and without 786-O cells were collected after 24 h and analyzed for the secretion of IFN-γ, TNF-α, granzyme B, Perforin, IL-2, and IL-10 by using the LEGENDplex multi-analyte flow assay kit (BioLegend).

Serial tumor challenge assay

B7H3.CAR-iNKT, B7H3-IL21.CAR-iNKT cells (2×10^5) and 786-O cells (2×10^5) were co-cultured in a 24-well plate by using fresh culture medium with 50 U/ml IL-2. After 2–3 days, iNKT cells were collected and counted using trypan-blue. The exhaustion markers of iNKT cells were analyzed by flow cytometry after every cycle. Then, CAR-iNKT cells were replated at an E:T ratio of 1:1 with fresh 786-O cells to start the next round tumor challenge.

Western blot assay

Harvested cells (CAR-iNKT co-cultured for 2h with 786-O cells) were washed two times with PBS, and protein lysates were shaken by using RIPA lysis buffer containing protease inhibitor, extracted on ice for 10 min, and centrifuged at 12,000 ×g for 20 min at 4°C. The protein concentration of this lysate was determined using the BCA protein assay kit (Thermo Fisher Scientific). Equivalent amounts of protein samples were separated by electrophoresis gels, and then transferred to an NC membrane. After blocking with 5% milk for 2 h, and the blots were incubated with primary antibodies STAT1, STAT5, pSTAT1, pSTAT3, pSTAT5 (Cell Signaling Technology), STAT1 and GAPDH (Proteintech). The membranes were washed three times and further incubated with a corresponding secondary antibody for 2 h at room temperature.

QUANTIFICATION AND STATISTICAL ANALYSIS

Statistical analysis was performed using GraphPad Prism 8 software. For comparisons between two groups, the two-sided unpaired or paired Student's t tests were used. One-way ANOVA was used for continuous variables among more than two groups. Survival was analyzed using the Kaplan-Meier method and the log rank test for between group comparison. All analysis and graphics show standard error of the mean bars (SD) and p values < 0.05 were considered to be statistically significant.